Supplemental Materials

Epsin nanotherapy regulates cholesterol transport to fortify atheroma regression

Kui Cui[1]†, Xinlei Gao[2]†, Beibei Wang[1]†, Hao Wu[1], Kulandaisamy Arulsamy[2], Yunzhou Dong[1], Yuling Xiao[3], Xingya Jiang[3], Marina V. Malovichko[4], Kathryn Li[1], Qianman Peng[1], Yaowei Lu[1], Bo Zhu[1], Rongbin Zheng[2], Scott Wong[1], Douglas B. Cowan[1], MacRae Linton[5], Sanjay Srivastava[4], Jinjun Shi[3], Kaifu Chen[2*], Hong Chen[1*]

†These authors contributed equally to this work.

*Corresponding authors. Email: hong.chen@childrens.harvard.edu

kaifu.chen@childrens.harvard.edu

The supplemental materials include:

MATERIALS and METHODS

Animal models

In this study, all animal procedures were performed in compliance with institutional guidelines and mouse protocols were approved by the Institutional Animal Care and Use Committee (IACUC) of Boston Children's Hospital, MA, USA. Both male and female mice were used. C57BL/6 mice (stock #00664), ApoE$^{-/-}$ mice (stock #002052), LysM-Cre deleter mice (stock #004781), and ABCG1^{flox} mice (C57BL/6-Abcg1^{tm1Ched}/J, stock #027954) were all purchased from Jackson Research Laboratory. As double knockout mice of Epsins 1 and 2 (Epsin1$^{-/-}$;Epsin2$^{-/-)}$ lead to embryonic lethality, we generated conditional Epsin1$^{fl/fl}$;Epsin2$^{-/-}$ mice previously described [19,20,23]. ApoE$^{-/-}$ mice, LysM-Cre$^{+/-}$ mice and Epsin1$^{fl/fl}$;Epsin2$^{-/-}$ mice were backcrossed to C57BL/6 background. We bred Epsin1$^{fl/fl}$; Epsin2$^{-/-}$ mice with LysM-Cre$^{+/-}$ mice to generate Epsin1$^{fl/fl}$; Epsin2$^{-/-}$; LysM-Cre$^{+/-}$ myeloid-specific Epsins deficient (LysM-DKO) mice (Figure S1B-a)[26]. **The detailed information of all the mice used in this study were described in Figure S1B.** These mice only have one copy of LysM Cre as homozygous LysM Cre mice are susceptible to atherosclerosis. In addition, we bred Epsin1$^{fl/fl}$; Epsin2$^{-/-}$; LysM-Cre$^{+/-}$ mice with ApoE$^{-/-}$ (C57BL/6) background to generate Epsin1$^{fl/fl}$; Epsin2$^{-/-}$; LysM-Cre$^{+/-}$; ApoE$^{-/-}$ mice (LysM-DKO/ApoE$^{-/-}$) (Figure S1B-b). Furthermore, we bred Epsin1$^{fl/fl}$; Epsin2$^{-/-}$; LysM-Cre$^{+/-}$; ApoE$^{-/-}$ (LysM-DKO/ApoE$^{-/-}$) mice with ABCG1$^{flox/+}$ to generate Epsin1$^{fl/fl}$; Epsin2$^{-/-}$; LysM-Cre$^{+/-}$; ABCG1$^{flox/+}$; ApoE$^{-/-}$ mice (LysM-DKO/ABCG1$^{flox/+}$/ApoE$^{-/-}$) (Figure S1B-c)**.** We also bred ABCG1$^{flox/+}$ with ABCG1$^{flox/+}$ to generate ABCG1$^{flox/flox}$ mice, then further bred ABCG1$^{flox/flox}$ mice with LysM-Cre$^{+/-}$ mice to generate ABCG1$^{flox/flox}$; LysM-Cre$^{+/-}$ (ABCG1 KO) (Figure S1B-d)**.**

The control mice for Epsin1$^{fl/fl}$; Epsin2$^{-/-}$; LysM-Cre$^{+/-}$ (LysM-DKO) mice were Epsin1$^{+/+}$; Epsin2$^{+/+}$ LysM-Cre$^{+/-}$ mice (WT) (Figure S1B-a). The control mice for Epsin1$^{fl/fl}$; Epsin2$^{-/-}$; LysM-

Cre$^{+/-}$; ApoE$^{-/-}$ (LysM-DKO/ApoE$^{-/-}$) were Epsin1$^{+/+}$; Epsin2$^{+/+}$; LysM-Cre$^{+/-}$; ApoE$^{-/-}$ (WT/ApoE$^{-/-}$) (Figure S1B-b). The control mice for Epsin1$^{fl/fl}$; Epsin2$^{-/-}$; LysM-Cre$^{+/-}$; ABCG1$^{flox/+}$; ApoE$^{-/-}$ mice (LysM-DKO/ABCG1$^{flox/+}$/ApoE$^{-/-}$) were Epsin1$^{+/+}$; Epsin2$^{+/+}$; LysM-Cre$^{+/-}$; ApoE$^{-/-}$ (WT/ApoE$^{-/-}$)(Figure S1B-c). The control mice for ABCG1$^{flox/flox}$; LysM-Cre$^{+/-}$ (ABCG1 KO) were ABCG1$^{+/+}$; LysM-Cre$^{+/-}$ (Figure S1B-d).

We used peritoneal macrophages from WT and LysM-DKO mice on either normal background or ApoE$^{-/-}$ background. We have not seen significant differences in the results with these backgrounds (detailed information of the mice that we used were interpretated in each figure legend). Therefore, we referred to the macrophages from WT or ApoE$^{-/-}$/WT as WT macrophages and macrophage from LysM-DKO or LysM-DKO/AopE$^{-/-}$ as DKO macrophages.

We used these mice (male and female) and primary macrophages (peritoneal and bone marrow derived) isolated from them for this study.

To induce atherosclerosis, mice were fed Western diet (WD, Protein 17% kcal, Fat 40% kcal, Carbohydrate 43% kcal; D12079B, Research Diets, New Brunswick, USA) starting at the age of 6-8 weeks for 8-20 weeks. Mice were sacrificed at different time points based on the experimental design and peritoneal macrophages, blood, heart, aorta and bone marrow monocytes were harvested. For control mice, in addition to ApoE$^{-/-}$;Epsin1$^{+/+}$;Epsin2$^{+/+}$ mice, we also used ApoE$^{-/-}$;Epsin1$^{+/+}$;Epsin2$^{+/+}$ mice with a single copy of LysM-cre, and ApoE$^{-/-}$;Epsin1$^{fl/fl}$;Epsin2$^{-/-}$ littermates lacking the single copy of LysM-cre. To simplify the terminology, we refer to these control mice as ApoE$^{-/-}$, as results were not different in any of the analyses we performed. For the study of atheroma resolution, WT mice (both male and female) at the age of 8 weeks were intravenously injected with $2x10^{11}$ genomes of PCSK9 adeno-associated virus (rAAV8-D377Y-mPCSK9 purchased from Boston Children's Hospital Viral Core Facility) followed by 17 weeks

of WD feeding. For each experimental model and time point, 6-10 mice were analyzed and both male and female mice were used in separate groups. In the current study, we did not exclude any mice when analyzing.

Aortic single-cell preparation and single-cell RNA (scRNA) sequencing

WT and DKO mice were euthanized by CO2 inhalation. The aortas were isolated after perfusion with 30 mL of PBS through left ventricular and quickly transferred to cold DMEM medium. Aortas from the two groups were cut into about small pieces and digested with an enzyme solution (5mg/mL collagenase type I, 5mg/mL collagenase type IV, and 5mg/mL liberase) for 90min at 37 °C on a shaker. The digested cell suspension was filtered through a 40 μm strainer and washed twice with PBS. The cells were resuspended and ready for sequencing in PBS with 0.04% bovine serum albumin, and their viability was over 90%.

Single-cell RNA-Seq library construction was performed using the protocol provided by 10X Genomics. In brief, the single-cell suspensions from both groups, reagents, gel beads and partitioning oil were loaded to 10X Chromium Chip G to generate single-cell Gel Beads-in-emulsion (GEMs, Single cell 3' Reagent Kits v3.1, 10X Genomics). scRNA was barcoded through reverse transcription in individual GEMs followed by a post GEM-RT cleanup and cDNA amplification. Then, a 3'-gene expression library construction was performed. Finally, the library was sent for sequencing.

ScRNA-seq data analysis and metabolite-sensor communication inference

The raw scRNA-seq data were processed using Cell Ranger (version 6.1.2) (10x Genomics). The reads were mapped to the prebuilt mouse mm10 genome. The resulted gene expression matrix in individual single cells was processed by the R package Seurat (version 4.1.0) [80]. Low-quality cells with number of expressed genes less than 200 or larger than 5000 or with percentage of

mitochondria reads greater than 10% were dropped out. Rarely expressed genes which were detected in less than 3 cells were removed. Mitochondria genes and ribosomal protein coding genes were removed from the expression matrix before normalization. The high-quality data after these filtering steps was then used at additional processing steps including log normalization, data scaling, principal component analysis (PCA), cell clustering, and UMAP visualization. The UMAP visualization of cell clusters was performed by the DimPlot function. Differentially expressed genes among cell clusters were identified by FindAllMarkers function using the default Wilcoxon test method, with minimal percentage of expressed cells as 25% and minimal log2 fold change as 0.25. Next, marker genes in each cell clusters were used to annotate cell types based on known marker genes in PanglaoDB database [50] and literatures. The marker gene expressions were visualized by DotPlot and VlnPlot function. Trajectory analysis was conducted by Monocle3 [81,82]. The metabolite-sensor cell-cell communication was analyzed by MEBOCOST [53]. The data was analyzed following the tutorial on the MEBOCOST website (https://github.com/zhengrongbin/MEBOCOST). Note that a metabolomics analysis was not conducted in this study. Instead, scRNA-seq expression data was used to estimate metabolite abundance and calculate communication score for each condition. Next, results of two conditions were combined to compare the communications. The differences in communication scores between two conditions were calculated. The prediction of sender-metabolite-sensor-receiver communication events were visualized by barplot, flow plot and circle plot. The metabolite abundance and sensor expression levels were exhibited by violin plot. Index of dispersion (IOD) was calculated using communication scores across conditions as described in the MEBOCOST paper[53]. The top 100 most variable communications were selected for further investigation. All the data for scRNA-seq are available in Data files (S1-S4).

Human samples

Human healthy control and diseased aortic arch samples from atherosclerosis patients were purchased from Maine Medical Center Biobank. The medical information of the atherosclerotic patient and healthy people samples is in Table S1. The paraffin sections were de-paraffinized and performed antigen retrieval to unmask the antigenic epitope with 10mM Sodium Citrate, pH 6.0, with 0.5% Tween 20 at 90°C for 10 minutes. Immunofluorescence staining of the slides was performed with the standard protocol described below.

Synthesis of DSPE-PEG-S2P, preparation and characterization of S2PNP-siRNA

To construct the lesional macrophage-targeted siRNA NPs, S2P peptide-conjugated DSPE-PEG (DSPE-PEG-S2P) was first synthesized via a thiol-maleimide Michael addition click reaction between S2P peptide (CRTLTVRKC, GLS Biochem Systems Inc.) and DSPE-PEG-Mal [PEG molecular weight, 3.4 kDa; Nanocs Inc.], as reported previously [59]. Then, a robust self-assembly method was used to prepare the targeted polymer-lipid hybrid NPs for siRNA delivery [59,83]. In brief, G0-C14 and PLGA were dissolved separately in anhydrous dimethylformamide (DMF) to form a homogeneous solution at the concentration of 2.5 mg/mL and 5 mg/ml, respectively. DSPE-PEG-OCH3 (DSPE-mPEG) and DSPE-PEG-S2P were dissolved in HyPure water (GE Healthcare Life Sciences, catalog no. SH30538) at the concentration of 0.1 mg/mL. 1 nmol Epsin1 siRNA and 1 nmol Epsin2 siRNA were gently mixed with 100 μL of the G0-C14 solution. The mixture of siRNA and G0-C14 was incubated at room temperature for 15 min to ensure the full electrostatic complexation. Next, 500 μL of PLGA polymers were added and mixed gently. The resultant solution was subsequently added dropwise into 10 mL of HyPure water containing 1 mg lipid-PEGs (i.e., 50% DSPE-PEG-S2P and 50% DSPE-mPEG hybrids for the S2P-targeted siRNA NPs, or 100% DSPE-mPEG for the non-targeted siRNA NPs) under magnetic stirring (1,000 rpm) for

30 min. The siRNA NPs were purified by an ultrafiltration device (EMD Millipore, MWCO 100 kDa) to remove the organic solvent and free excess compounds via centrifugation at 4 °C. After washing 3 times with HyPure water, the siRNA NPs were collected and finally resuspended in pH 7.4 PBS buffer. The NPs were used freshly or stored at -80 °C for further use. The physicochemical properties (particle size and surface charge) of S2PNP-siEpsin1/2 were characterized by dynamic light scattering (DLS, Brookhaven Instruments Corporation). The S2PNP-siEpsin1/2 was ~89 nm in size as measured by DLS, and their surface charge was determined to be ~ -5.3 mV.

Isolation of primary mouse macrophage and macrophage culture

The isolation of peritoneal macrophages was performed as described previously [84]. Briefly, mice were intraperitoneally injected with 1mL of 4% thioglycolate (TG), and 3 days post-injection, mice were sacrificed, and peritoneal cells were harvested with 7mL of sterile PBS by lavage of peritoneal cavity. Cells were spun down (1000xg, 5 minutes), washed with PBS, resuspended, and plated in RPMI (containing 10% FBS and 1% Pen-Strep) at 37 °C in humidified air containing 5% CO_2 atmosphere. After 3 hours, non-macrophages were washed with PBS. For bone marrow-derived macrophages, mice were sacrificed, and both femurs and tibias were dissected and flushed with sterile 1X PBS, followed by passing through a 70μM cell strainer. Cells were spun down (1000xg, 5 minutes), washed with PBS, and seeded in RPMI (containing 10% FBS and 1% Pen-Strep) with macrophage colony stimulating factor (M-CSF, 10ng/mL) to differentiate into macrophages for 5 days. After which, the macrophages were harvested and used in experiments. Both bone marrow-derived and isolated peritoneal primary macrophages were used to confirm knock out of Epsin1 and Epsin2. Isolated peritoneal macrophages were mainly used for western blots, flow cytometry and immunoprecipitations due to higher yields.

Human THP1 macrophage culture and transfection of Epsin1/2 siRNA mix

THP1 monocytes (human monocytic leukemia cell line) from ATCC (TIB-202) was cultured in RPMI 1640 medium containing 10% fetal bovine serum and 1% penicillin/streptomycin at 37^0C in 5% CO_2 humidified incubator. THP1 monocytes ($1X10^6$ cells/mL) were differentiated into THP1 macrophages with 10 ng/mL phorbol 12-myristate 13-acetate (PMA) for 48 hours. Then, the transfection of control siRNA (4 μg) and human epsin 1 and 2 siRNAs mix (2 μg/each siRNA) to the differentiated THP1 macrophages were performed using a Nucleofector 2b device for electroporation of the cells[85]. After transfection, the transfected THP1 macrophages were incubated with different kinds of compounds for functional studies.

RNA isolation, quantitative real-time PCR and RNA sequencing

Total RNA was extracted from primary macrophages with Qiagen RNeasy Mini Kit based on manufacturer's instruction including the optional step to eliminate genomic DNA. The extracted RNA was either used for qRT-PCR or RNA sequencing according to the experimental designs.

For qRT-PCR, mRNA was reverse transcribed to cDNA with the iScript cDNA Synthesis Kit (Bio-Rad Laboratories, Inc., Hercules, CA, United States). 2 μL of the product was subjected to qRT-PCR in StepOnePlus Real-Time PCR System (Applied Biosystems) using SYBR Green PCR Master Mix reagent as the detector. PCR amplification was performed in triplicate on 96-well optical reaction plates and replicated in at least three independent experiments. The ΔΔCt method was used to analyze qPCR data. The Ct of β-actin cDNA was used to normalize all samples. Primers are listed in Major Resource Table. For RNA sequencing, extracted RNA from primary macrophages with Qiagen RNeasy Mini Kit based on manufacturer's instruction were sent to BGI Genomics Company (San Jose, USA) for RNA sequencing.

RNA sequencing data processing and differential expression analysis

The raw reads of RNA sequencing data were mapped to the mouse genome (version mm10) using STAR (version 2.7.9a) [86] or TopHat (version v2.1.1) [87]. The read count was calculated for each gene by htseq-count (version 0.11.2) [88] and further normalized to TPM (transcripts per million) and FPKM (fragments per kilobase of transcript per million fragments mapped). For differential expression analysis of Epsin deficient and wild type macrophage dataset, the read count matrix produced by htseq-count was imported into the R package DESeq2 (version 1.30.1) [89]. For the ABCG1 knock out dataset, we first performed a batch effect removal on the log10 transformed TPM expression matrix using ComBat in the R package sva (version 3.38.0) [90]. Then, the R package limma was used to do differential expression analysis for the batch effect-removed expression matrix. Genes with fold change larger than 1.2-fold and p-value less than 0.05 were identified as differentially expressed genes (DEGs). Principal component analysis (PCA) was conducted by the plotPCA function of DESeq2. Heatmap of gene expression values was generated using the R package heatmap (version 1.0.12). Gene Ontology (GO) functional enrichment analysis was performed by the R package clusterProfiler (version 3.18.1) [91].

For the comparison of DEGs between DKO and CD36 knockout macrophages in mice, we utilized the published bulk RNA-seq data from Chen et. al. [56], with the accession number GSE139439, downloaded from NCBI GEO database [92]. The overlapping DEGs co-regulated in DKO and CD36 knockout macrophages were analyzed by the R package VennDiagram (version 1.6.20) [93]. The statistical significance of overlapping genes was calculated by Fisher exact test. All the data for bulk RNA-seq are available in Data files (S5-S16).

Cell culture and plasmids transfection

The HEK 293T cell line (ATCC no. CRL-11268) was used for plasmid transfection to map the binding sites of Epsin to CD36 or ABCG1. Flag-tagged Epsin1^{WT}, Epsin1$^{\Delta UIM}$, Epsin1$^{\Delta ENTH}$

truncation constructs, and pcDNA vector were prepared previously in our lab[25]. CD36 (lot:52025) and ABCG1 (lot:53952) plasmids were purchased from AddGene. HEK 293T cells were cultured in DMEM (10% FBS and 1% Pen-Strep) at 37°C in humidified air containing 5% CO_2 atmosphere and transfected using Lipofectamine 2000 as instructed by the manufacturer. Transfection of Epsin domains to macrophage: Isolated WT and DKO peritoneal macrophages were cultured in RPMI media (containing 10% lipid-depleted serum and 1% Pen-Strep). Epsin1^{WT}, Epsin1$^{\Delta UIM}$, Epsin1$^{\Delta ENTH}$ truncation constructs, and pcDNA vector were transfected to macrophages using lipofectamine LTX transfection reagent or using Nucleofector II apparatus (Amaxa, Germany) with mouse macrophage nucleofector kit (Lot: VPA-1009, Lonza) as instructed by the manufacturer.

Immunoprecipitation (IP) and western blotting (WB)

For total protein levels, primary macrophages were washed with ice cold PBS, lysed in RIPA buffer (50 mM Tris HCl, 150 mM NaCl, 1.0% NP-40, 0.5% Sodium Deoxycholate, 1.0 mM EDTA, 0.1% SDS and 0.01% sodium azide at a pH of 7.4.), added 4X Laemmli buffer (1:3 dilution in lysis buffer) was added and WB was performed for the proteins indicated in this study. For IP, cells were washed with ice cold PBS, lysed with lysis buffer (1% Triton X-100, 5mM Na_3VO_4, 10mM N-ethylmaleimide, and protease inhibitor cocktail), spun down (12000xg, 5 min at 4°C) to remove the debris. Cell lysates were pre-cleared with appropriate species of IgG and protein A/G Sepharose beads for 1h at 4°C with rotation followed by incubation with A/G Sepharose beads and indicated antibodies for 12 hours at 4°C with rotation. For negative controls, equal concentrations of mouse IgG were added instead of specific antibodies. Precipitated proteins were washed with ice cold lysis buffer for 3 time and eluted from protein A/G beads using 2X Laemmli buffer (1:1 in lysis buffer) followed by WB as described previously [26]. WB were repeated for at least 3 times with different mice and bands were quantified using NIH ImageJ software. The protein expression

levels were normalized to GAPDH levels. For IPs in macrophages involving oxLDL treatment, cells were pre-treated with 1 μM MG132 in serum-free media for 4 hours, followed by the treatment with or without oxLDL (100μg/ml) for 30 minutes at 37°C and processed for immunoprecipitation. For the transfection of Epsin1 constructs and CD36 or ABCG1 constructs, transfected HEK 293T cells were cultured in lipid-depleted DMEM media for 24 hours followed by stimulation with 100μg/mL oxLDL for 30 minutes at 37°C and performed for immunoprecipitation.

Atherosclerosis analysis

Mice were anesthetized with isoflurane. Blood was collected from the right atrium followed by left ventricle perfusion with cold PBS. Whole aortas, brachiocephalic artery (BCA) and hearts of the mice were isolated. Whole aortas were dissected symmetrically, pinned to parafilm and fixed in 4% PFA to allow the *en face* analysis. Heart and BCA were embedded in OCT mounting medium and immediately frozen. The aortic sinus and BCA in the heart were sectioned at 10 microns (at least 9 sections of each sample were collected). The internal elastic lamina and luminal boundary of the lesion was manually traced and the lesion sizes of the *en face* aortas and aortic roots were quantified by NIH ImageJ software. The methods for Oil Red O (ORO) staining, immunofluorescent (IF) staining, Hematoxylin and Eosin (H&E) staining, and Van Gieson's staining are described in supplemental materials [26].

ORO staining and IF staining of primary macrophages or cryosections were performed as described below. Oil Red O imaging was taken by a Zeiss Axio Scope.A1, AxioCam ICc5, and analyzed by ZEN-Lite 2012 software. Imaging of *en face* aortas was performed using a Nikon SMZ1500 stereomicroscope, SPOT Insight 2Mp Firewire digital camera, and SPOT Software 5.1. Imaging of IF staining was taken by Zeiss confocal microscope and quantification areas were

performed by manually tracing the aortas, BCA, and aortic root lesion areas with NIH ImageJ software. Statistical analysis of samples including Oil Red O, Van Gieson's, H&E, and IF staining were performed by blinding in which each animal was assigned a number and data was collected based on the assigned number with genotype and experimental condition unknown to the data collector.

Oil Red O staining

For cryostat sections: cryostat sections 10 microns were fixed in 4% paraformaldehyde. Slides were washed with PBS (3 times, 5 min each time), and rinsed with 100% propylene glycol followed by staining with freshly prepared 0.5% Oil Red O solution for 10 minutes at 60°C. Slides were then put in 85% propylene glycol for 2 min, followed by 3 washes in water. Slides were next incubated with hematoxylin for 1-2 min, rinsed 3 times in water, and mounted with aqueous mounting medium. For foam cells: coverslips were washed with PBS, fixed in 4% paraformaldehyde for 10 min and stained with freshly prepared 0.5% Oil Red O solution for 10 min at 65°C. Slides were then washed in PBS (3 times, 5min each time), incubated with hematoxylin for 1min, washed with PBS 3 times, and mounted on coverslips with aqueous mounting medium. Imaging was processed with a Zeiss LSM880 confocal microscope and analyzed with ZEN-Lite 2012 software and NIH ImageJ software. Quantification of lesion was performed as described above. Quantification of foam cells was performed as described below.

Hematoxylin and Eosin staining

Frozen aortic root and BCA sections: slides were fixed in 10% buffered formalin for 15 min and washed in water. Next, slides were stained with 0.1% hematoxylin for 3min followed by ddH_2O washes, 95% ethyl alcohol and water. Slides were then dipped in 0.5% Eosin for 3 min,

quickly rinsed with ddH_2O, dipped in 95% and 100% ethanol, incubated in 50:50 Xylenes:100% ethanol and incubated in 100% Xylenes. Slides were mounted using Permount with coverslips.

Van Gieson's staining

Sections were fixed in 10% buffered formalin for 15 min and washed in water. Slides were stained with hematoxylin for 10 min, washed in ddH_2O, stained 1-3 min in Van Gieson's solution, dehydrated in 95% alcohol and 100% alcohol two times. Then, slides were cleared in xylene for two times and mounted with Permount. Staining results were presented as: Elastic fibers and nuclei–Black, Collagen fibers–Red and Other tissue elements–Yellow. Lesion area was traced using NIH ImageJ software. The percentage of necrotic area was determined by necrotic areas within the lesion. Collagen content was determined by the percentage of lesion areas.

Immunofluorescence staining

Human samples: human healthy and atherosclerotic aorta paraffin sections were deparaffinized in xylene for 15min, immersed in graded ethanol (100%, 100%, 95%, 90%, 80%, and 70%, each for 3 min), washed with running tap water and processed antigen retrieval with 10mM Sodium Citrate, pH 6.0, with 0.05% Tween 20 at 90°C for 10 min. Samples were blocked in PBS with 3% donkey serum, 3% BSA, and 0.3% Triton X-100 and incubated with primary antibodies ABCG1 or CD68 (1:70 dilution) at 4°C overnight. The sections were washed three times and respective secondary antibodies conjugated to fluorescent labels (Alexa Flour 594, 488, or 647; 1:200 to 1:500) were added for 2 h at room temperature. The sections were mounted with mounting medium containing DAPI (1:100). Isotype controls for the immunofluorescence experiments was used to validate antibody specificity (isotype antibodies) and distinguish genuine target staining from background (secondary antibody only controls).

Mouse aortic root and BCA cryosections: Sections were fixed by 4% paraformaldehyde for 30 min at room temperature and blocked in PBS solution containing 3% donkey and/or goat serum, 3% BSA, and 0.3% Triton X-100 for 1hour. Samples were then incubated with primary antibody at 4°C overnight, followed by incubation with the respective secondary antibodies conjugated to fluorescent labels (Alexa Flour 594, 488, or 647; 1:200 to 1:500) for 2 h at room temperature. The sections were mounted with mounting medium containing DAPI (1:100).

Staining of peritoneal macrophages: macrophages plated on the 18-mm coverslips were washed with PBS, fixed by 4% paraformaldehyde for 15 min at room temperature and blocked in PBS solution containing 3% donkey and/or goat serum, 3% BSA, and 0.3% Triton X-100 for 1hour. Coverslips were then incubated with primary antibody (CD36, ABCG1, EEA1, Rab11, or Lamp1; 1:100-1:300) at 4°C overnight, followed by incubation with the respective secondary antibodies conjugated to fluorescent labels (Alexa Flour 594, 488, or 647; 1:200 to 1:500) for 1 hour at room temperature. The sections were mounted with mounting medium containing DAPI (1:100). BODIPY™ 493/503 staining of macrophages was performed following F4/80-fluorescent conjugated antibody incubation for 2 hours at room temperature [94]. Slides were washed with PBS, stained with DAPI and mounted. Immunofluorescent images were captured using a Zeiss LSM880 confocal microscope and analyzed with ZEN-Lite 2012 software and HIH ImageJ software. Samples stained without the primary antibody were obtained using the same settings as negative controls. Mean fluorescence intensity (MFI) of antibody staining was determined using NIH ImageJ software with n=3 or more.

Image Choosing

We had two blinded observers select representative images from a panel of images collated from all experiments performed for any given sample. Representative images from

immunofluorescence, Oil Red O and Van Gieson's staining were selected based on and the most accurate representation of similarity with the mean value for each experimental group. The way to select a representative image would be an image that is most similar to all of the other images in the set. Representative images from immunofluorescence, Oil red O and Van Gieson's stainings were selected based on high quality, resolution, and accurate representation of similarity with the mean value for each experimental group.

Flow cytometry assay

Flow cytometry of elicited primary macrophages: peritoneal macrophages from WT and DKO mice were isolated as described above and plated in 6 well plates in lipid-deficient medium for 24 hours followed by the treatment with or without 100μg/mL oxLDL in the presence or absence of clathrin siRNA at 37^0C for different time based on the experiment designs. Macrophages were washed with 1XPBS, dissociated with 1mL non-enzymatic cell dissociation buffer, centrifuged (300x*g*, 5 minutes), and resuspended in 100μL FACS buffer (1X PBS, 2% FBS, 2mM EDTA) containing the following: FcR Blocking Reagent, fluorochrome conjugated anti-F4/80, primary antibodies against CD36 or ABCG1. Cells were incubated with the primary antibodies (1:100) on ice for 30min, washed with 100μL FACS buffer, spun down and resuspended with 100μL FACS buffer containing the fluorescent secondary antibodies (1:100). After 30 min, cells were washed with FACS buffer, fixed with 4% paraformaldehyde (PFA), and resuspended in FACS buffer for analysis. Single color and no color controls were prepared using elicited macrophages, which were treated the same as experimental groups. Expression of cell markers was analyzed using a FlowJo version 10 software. Gating strategies were performed as described in Supplemental Figures S4 and S10. Flow cytometry of DiI-oxLDL treated macrophages: peritoneal macrophages elicited from WT and DKO mice were incubated in lipid-deficient medium for 24h followed by the

treatment of DiI-oxLDL for 2h at 37^{0}C and macrophages were washed with 1XPBS, dissociated with 1mL non-enzymatic cell dissociation buffer, centrifuged (300xg, 5 minutes), resuspended in 100μL FACS buffer (1X PBS, 2% FBS, 2mM EDTA) containing the following: FcR Blocking Reagent, fluorochrome conjugated anti-F4/80 antibody staining, fixed and assessed the uptake of lipoproteins by flow cytometry as described above.

Foam cell formation

TG (4%) induced peritoneal macrophages were isolated and plated on 18mm glass coverslips. Cells were cultured in RPM media (containing 10% lipid-depleted serum and 1% PennStrep) for 24 hours and then treated with 10-100 μg/mL oxLDL for 24 hours [26]. Cells were fixed in 4% PFA for 10 minutes at room temperature and washed with PBS. For Oil Red O staining, coverslips were stained with Oil Red O, washed with PBS, counterstained with hematoxylin, washed with PBS, and then mounted on slides. For Bodipy staining, coverslips were immunofluorescently stained BodipyTM 493/503 and phalloidin-iFluor 555 reagent for 1 hour at 37°C, counterstaining with DAPI, and mounting on slides. Negative controls were not treated with oxLDL. Foam cells were determined as the number of lipid positive cells (Oil Red O positive or Bodipy positive) as a percentage of total cells. At least 6 fields per cover slip and 6 mice per genotype were used for quantification.

Cell surface biotinylation

Cell surface biotinylation was performed as described previously [26]. Isolated peritoneal macrophages in the plate were washed with cold PBS, suspended at a concentration of 25x10^6 cells/mL and treated with 2mM EZ-Link Sulfo-NHS-LC-Biotin reagent on ice for 30 minutes followed by 3 washes with 100mM Glycine to remove excess biotin and then 3 washes with cold

PBS (5min each time). Cells were lysed and pulled down by streptavidin bead: cell lysates were incubated with neutravidin beads for at least 12 hours at 4°C with rotation, and proteins were eluted from beads using 4X Laemmli buffer diluted 1:3 in lysis buffer. Cell surface biotinylated proteins were analyzed by western blotting and quantified using NIH Image J software.

Plasma collection, triglyceride, and cholesterol analysis

For each mouse, 1mL syringe were rinsed with 1mL 0.5M EDTA to coat the inside of the syringe with EDTA to prevent clotting during blood collection. Blood was collected from the right atrium of the mouse heart after sacrifice with isoflurane and added to each 1.7mL tube containing 50μL 0.5M EDTA. Blood was centrifuged at 2000xg for 10 minutes at 4°C. Plasma was transferred to a new tube and stored at -20°C. Plasma cholesterol and triglyceride levels were determined as described below.

Total cholesterol, high-density lipoprotein (HDL) cholesterol and triglycerides in mouse serum were determined on Ace Axcel Clinical Chemistry System (Alfa Wassermann, West Caldwell, NJ). Non-HDL cholesterol is calculated as Total Cholesterol – HDL and gives a measure of the cholesterol carried by all of the atherogenic lipoproteins.

Quantification of total cholesterol, HDL and triglycerides in macrophages. Lipids were extracted from macrophages with hexane:isopropanol (3:2, v:v) as described in Robinet et al [95]. Solvents were removed by drying with nitrogen gas. Extracts were resolubilized in 5% bovine serum solution by bath sonication (10 minutes at 37°C), freeze/thaw treatment (1 hour at -80°C) and followed by probe sonication for 10 seconds. Reconstituted samples were analyzed on Ace Axcel® Clinical Chemistry System for total cholesterol, HDL and triglycerides as described above for measurements in mouse serum. Obtained values were normalized to total protein measured in the cell lysates by Bradford Protein Assay (Bio-Rad).

Macrophage cholesterol efflux assay

Thioglycolate induced peritoneal macrophages from WT, DKO and DKO/ABCG1$^{fl/+}$ mice were plated in RPMI medium for 2-4 hours. Non-adherent cells were removed by washing with PBS and cells were incubated with radiolabeled medium supplemented with 4 μCi/mL of [^{3}H]-cholesterol (Perkin-Elmer, Waltham, MA, USA), 5% FBS,1% P/S and 50μg/mL acetyl-LDL for 24 hours. Macrophages were washed twice with warm PBS and incubated with serum-free RPMI 1640 medium supplemented with 0.2% BSA, 2μg/mL acyl-CoA cholesterol acyltransferase (ACAT) inhibitor and 4μmol/L LXR agonist T0901317 for 18 hours equilibration [58]. After this equilibration period, cells were washed twice with warm PBS and incubated in serum free RPMI medium supplemented with or without cholesterol acceptors (10 μg/mL ApoA-1 or 25 μg/mL HDL) and 2μg/mL ACAT inhibitor for 4 hours [96]. At the end of the incubation, the efflux media was collected and filtered through a 0.45-μm filter to remove the detached cells. Then, transfer the efflux medium was transferred to a scintillation vial. The macrophages in the plates were added to 500 μL of 0.2N NaOH and incubated on shaker at 4 °C overnight. Cell extract from each well was transferred to a scintillation vial. 4 mL of scintillation liquid were added to each scintillation vial and radioactivity was measured by liquid-scintillation counting [97]**.** The cholesterol efflux to acceptors was expressed as a percentage of total cholesterol using the following formula: % cholesterol efflux = (medium [^{3}H]-radioactivity [cpm]) / [(medium [^{3}H]-radioactivity [cpm] + [^{3}H]-radioactivity from cell extract [cpm])] x 100, where cpm = counts per minute.

Reverse cholesterol transport (RCT) assay

In vivo RCT experiment is based on the method detailed by Joan Carles Escolà-Gil et al [97]. Briefly, macrophages were radiolabeled with [^{3}H]-cholesterol (5 μCi/mL) in 10% lipoprotein-depleted serum, 1% P/S and 50μg/mL acetyl-LDL RPMI media for 48h. Foam cells were washed

with serum-free media supplemented with 0.2% BSA and equilibrated for 4h (37 °C, 5 % CO_2). Then, [^{3}H]-cholesterol-labeled macrophages were detached, spun down and resuspended in PBS. The injection dose was 0.5 mL per mouse ($4x10^6$ cpm/mL) administered intraperitoneally into C57BL/6 WT mice fed on normal diet as indicated in Figure 5C. Mice were then individually housed in metabolic cages and feces in the cage floor were collected for 2 days. At 48h, mice were sacrificed and blood, liver, intestinal contents were collected in Figure S8. Serum [^{3}H]-cholesterol was measured by liquid scintillation counting. [^{3}H]-HDL cholesterol was determined after precipitation of ApoB-containing lipoproteins with 0.44mM phosphotungstic acid and 20mM $MgCl_2$. Liver, fecal and intestinal lipids were extracted with hexane- isopropanol (3:2, v:v) and partitioned against Na_2SO_4. The lipid layer was collected and dried for 48h using nitrogen gas in a fume hood, and [^{3}H]-cholesterol radioactivity was measured by liquid scintillation counting (4mL scintillation fluid for 4 min). The [^{3}H]-radioactivity observed in fecal biliary acids was determined in the remaining aqueous phase of fecal material extracts. The amount of [^{3}H]-radioactivity was expressed as a percentage of the total injected dose, which was taken as 100%.

Statistical analysis

Statistical analysis was processed using GraphPad Prism 9.3 and IBM SPSS Version 26. Data are shown as mean ± standard deviation (mean ± SD). For in vitro study, all biological replicates using primary cultured cells or cells lines correspond to independent experiments from distinct expansions and passage numbers, with technical replicates. Shapiro-Wilk test ($P<0.05$) was used to test normality of all data obtained from in vivo study. Comparisons among multiple groups were performed using one-way analysis of variance (ANOVA) followed by Tukey post hoc multiple comparisons test or two-way ANOVA followed by Sidak post hoc multiple comparisons test. For comparisons between two groups, unpaired *t* test was performed to analyze the data. Data that

failed normality test or small sample size (n<6 per group), Mann-Whitney *U* test were used to analyze two-group comparisons and Kruskal-Wallis followed by Dunn post hoc multiple comparisons test for multi-group comparisons. Raw P values were provided for two-group comparisons, and adjusted P values were provided for multiple-group comparisons. All experiments were performed independently, no experiment-wide/across-test multiple test correction was applied.

Supplemental Figure Legends

Figure S1A. Overview of single cell RNA sequencing (scRNA-seq) and data analysis. **Sample preparation**: WT and DKO mice (n=3/group) were fed normal diet or western diet for 16 weeks, followed by the isolation of aortas, enzyme digestion and single cell suspension were prepared by manufacturer's instructions. **10X Genomics- Single-cell cDNA library preparation**: barcoding cells for 10 x genomics, cDNA library construction and scRNA sequencing. **cDNA library sequencing and computational analysis:** Then the sequencing reads were preprocessed by cell ranger, downstream analysis was done by Seurat, Scanpy, and Monocle pipelines.

Figure S1B. **Overview of animal models.** (**a**) Generating myeloid-specific Epsin deletion mice. (**b**) Generating myeloid-specific Epsin deletion mice in ApoE$^{-/-}$ background. (**c**) Generating LysM-DKO/ABCG1$^{flox/+}$ in ApoE-null mouse. (**d**) Generating ABCG1 knockout mice.

Figure S2. Cell populations were annotated based on marker gene expression. (**A**) Dot plot of known marker genes for each cell cluster in Figure 1A. Marker gene expression are colored by red and blue for aortas in WT and LysM-DKO mice on normal diet, respectively. Size of nodes represent percentage of cells expressing a certain gene. (**B**) Dot plot of known marker genes for each major macrophage subcluster. (**C**) Violin plots showing the representative marker gene expression in each major macrophage subcluster in WT and LysM-DKO. (**D**) Feature plots showing the representative M1 and M2 macrophage marker gene expression across all major macrophage subclusters. Log-transformed normalized read count: Read counts for each cell were divided by the total counts for that cell and multiplied by 10,000. This was then natural log transformed using log1p.

Figure S3. Cell proportion changes for each cell type in WT and LysM-DKO. The bar plots showing the cell proportion of M1 macrophage was decreased, while those of M2 macrophage and M1-M2 transition cells were increased in LysM-DKO compared to WT.

Figure S4. Metabolite-sensor cell communications related to macrophages. (**A-B**) A flow plot of communications comprising senders, metabolites, sensors, and receivers from macrophage subpopulations to all the cell types (A); and from all cell types to macrophages (B). (**C**) A heatmap showing the most variable communications related to cholesterol metabolism in macrophages in the comparison of WT and LysM-DKO aorta.

Figure S5. The expression levels of cholesterol-producing enzymes and the sensor Cd36 tended to decrease while those of cholesterol-consuming enzymes tended to increase in DKO compared to WT mice. (**A**) Violin plots showing the expression levels of cholesterol producing enzymes in DKO and WT macrophage c2. (**B**) Violin plots showing the expression levels of cholesterol consuming enzymes in DKO and WT macrophage c2. (**C**) Dot plot showing the expression levels of cholesterol producing enzymes in DKO and WT macrophage c2. (**D**) Dot plot showing the expression levels of cholesterol consuming enzymes in DKO and WT macrophage c2. (**E**) Violin plot showing the expression level of Cd36 in DKO and WT M1-M2 transition cells. Log-transformed normalized read count: Read counts for each cell were divided by the total counts for that cell and multiplied by 10,000. This was then natural log transformed using log1p.

Figure S6. The expression levels of the producing and consuming enzymes for 25-hydroxycholesterol in macrophage subpopulations in WT and DKO aorta. (A) Violin plots showing the expression levels of 25-hydroxycholesterol producing and consuming enzymes across macrophage subpopulations in WT and DKO. (**B**) Dot plots showing the expression levels of 25-hydroxycholesterol producing and consuming enzymes across macrophage subpopulations in WT and DKO. Log-transformed normalized read count: Read counts for each cell were divided by the total counts for that cell and multiplied by 10,000. This was then natural log transformed using log1p.

Figure S7. RNA-seq analysis of WT and DKO macrophages reveals that Epsins regulate lipid cholesterol metabolism and efflux pathways. (**A**) A volcano plot showing differential gene expression in Epsin deficient (DKO) and wild type (WT) macrophages. Red and blue indicate up- and down-regulated genes, respectively. (**B**) A heatmap showing the expression of genes involved in the cholesterol metabolic process (GO:0008203) and cholesterol efflux (GO:0033344). (**C-E**) GSEA demonstrated the tendency of individual pathways to be up- or down- regulated in Epsin deficient macrophages compared to wild type (top panels). Genes associated with Fatty acid metabolism (HALLMAKR) (C), NR1H3-NR1H2 regulate gene expression linked to cholesterol transport and efflux (Reactome) (D), and negative regulation of macrophage derived foam cell differentiation (GOBP) (E) are analyzed. The bar plots (bottom panels) showing log2 fold change of altered genes in these pathways. (**F**) Venn diagrams (top panels) showing the number of overlapping up- and down-regulated genes in DKO and CD36 knockout (CD36KO) samples. Bar plots (bottom panels) showing the observed numbers of overlapped genes versus numbers expected by random chance. The P-value was calculated using two tail Fisher exact test. (**G**) The Gene Ontology (GO) enrichment analysis for shared down regulated (top) and up regulated genes (bottom) between DKO and CD36KO macrophages. * Adjusted $P<0.05$, ** adjusted $P<1x10^{-5}$. For comparison between different genes, the log-transformed values were further scaled using Z-score method.

Figure S8. Gating strategy and clathrin-mediated CD36 internalization. (**A**) Macrophages isolated from WT (n=6) and DKO (n=6) mice were incubated in lipid-deficient medium for 24h followed by treatment with oxLDL for 2h, then staining with CD36-Alex488 and cytometric analyses. (**B**) Macrophages isolated from WT (n=6) and DKO (n=6) mice were incubated in lipid-deficient medium for 24h followed by the treatment of 10 μg/mL Dil-oxLDL for 2h at 37^0C and assessed the uptake of lipoproteins by flow cytometry. The major macrophage population was selected in forward vs side scatter plots and single cell determination was performed by FSC-H vs FSC-A. CD36 (A) or DiI-oxLDL (B) positive macrophages were presented in Figure 2C and 2H, respectively. (**C**) WT and DKO macrophages were incubated in lipid-deficient medium and transfected with clathrin siRNA for 24h followed by treatment with or without 100μg/mL oxLDL for 15 mins at 37^0C. Flow cytometry for surface level of CD36.

Figure S9. The loss of Epsins reduced oxLDL uptake by macrophages. (**A**) Isolated peritoneal macrophages from WT (n=6) and DKO (n=6) mice were pre-incubated with 25μg/mL oxLDL for 24h in lipid-deficient medium and stained with BODIPY (lipids, green), F4/80 (macrophage, red), and DAPI (blue), **WT vs DKO group, n=6, $P<0.01$, scale bar=200μm. (**B**) ORO staining of

peritoneal macrophages, which were pre-incubated with 25μg/mL oxLDL for 24h in lipid-deficient medium, scale bar=20μm.

Figure S10. Transfection of full-length Epsin1 and constructs with the ENTH and UIM domains deleted into WT macrophages did not affect lipid uptake. Constructs of FLAG-Epsin1 WT, ΔENTH, and ΔUIM were transfected into $ApoE^{-/-}$/WT macrophages for 48h and treated with 100 μg/mL oxLDL for 1h, followed by staining with F4/80 (red), BODIPY (green) and DAPI (blue). Scale bars=200μm. Statistical analyses are presented in Figure 3E.

Figure S11. Differentially expressed genes between WT and ABCG1 knockout (ABCG1KO) macrophages. (**A**) A volcano plot showing differential gene expression in ABCG1KO and WT macrophages. Red and blue indicate up- and down-regulated genes, respectively. (**B**) A heatmap exhibiting the expression values of up- and down-regulated genes in each sample. (**C**) Bar plots showing log2 fold changes of the top 30 up- and down-regulated genes between ABCG1KO and WT macrophages. Up- (red) and down-regulated (blue) genes are indicated. (**D**-**F**) GSEA (top panels) indicated the tendency of individual pathways to be up- or down-regulated in response to DKO or ABCG1KO compared to WT cells. Genes associated with cell activation involved in immune response (GO:0002263) (D), regulation of leukocyte migration (GO:0002685) (E), and leukocyte proliferation (GO:0070661) (F) were analyzed. The bar plots (bottom panels) showing log2 fold change of altered genes in these pathways. For comparison between different genes, the log-transformed values were further scaled using Z-score method.

Figure S12. Schematic of the quantification for radiolabeled cholesterol. [^{3}H]-cholesterol was measured in serum and HDL after precipitating ApoB-containing lipoproteins. Liver, feces and intestinal lipids were extracted with hexane–isopropanol and partitioned against Na_2SO_4. Liver [^{3}H]-radioactivity was determined in the upper layer, which contains the [^{3}H]-cholesterol. In the feces extract, the amount of [^{3}H]-radioactivity was determined in the upper layer (neutral sterols) and the lowest layer (bile acids). In the intestinal contents, [^{3}H]-radioactivity was determined in the upper layer.

Figure S13. Gene expression levels of indicated genes in WT and DKO macrophage. Peritoneal macrophages were isolated from WT (n=5) and DKO (n=5) mice. Total RNA was extracted and mRNA levels of ABCG1, Epsin1, and Epsin2 were measured (n=5/group).

Figure S14. Gating strategy and clathrin mediated-ABCG1 endocytosis. (**A**) Macrophages isolated from WT and DKO mice were incubated in lipid-deficient medium and treated with LXR agonist for 24h followed by treatment with or without 100 μg/mL oxLDL for 5min, 15min, and 45min, and then stained with ABCG1. Surface levels of ABCG1 were assessed by flow cytometry. The major macrophage population was selected in forward versus side scatter plots and single cell determination was performed by FSC-H vs FSC-A. Isotype controls were gated in the histogram as M1 for the negative control of experimental groups for Figure 6C. (**B**) Statistical analysis is presented for Figure 6C. At least three independent experiments were performed for statistical analysis. Data are presented as mean ± SD. **(C)** WT and DKO macrophages were incubated in lipid-deficient medium and transfected with clathrin siRNA for 24h followed by treatment with or without 100μg/mL oxLDL for 15 mins at 37^{0}C. Flow cytometry for surface level of ABCG1.

Figure S15. The expression of ABCG1 decreased with progression of atherosclerotic lesions in humans and mice. (**A-B**) Immunostaining of CD68 (red), ABCG1(green) and DAPI (blue) of human patient aortic arch sections (A, n=6) and mouse aortic root sections (B, n=6) in early and advanced stage of atherosclerosis （white dashed line outlined in CD68). Mean fluorescence intensity (MFI), scale bar, A=50μm, B=200μm.

Figure S16. Characterization and silencing efficacy of S2P-conjugated siEpsin1/2 NPs. (**A**) Schematic of the targeted hybrid siRNA NP platform composed of a lipid-PEG shell with a lesion macrophage specific targeting ligand, S2P peptide, and a PLGA core. (**B-C**) Macrophages from WT mice were treated with S2PNP-siCtrl or S2PNP-siEpsin1/2 for 24h, RNA and proteins were isolated, qRT-PCR (B) and western blot (C) was performed to check the expression of Epsin 1 and 2 levels (n=3).

Figure S17. S2PNP-siEpsin1/2 treated macrophages show reduced foam cell formation. (**A-B**) Macrophages isolated from ApoE$^{-/-}$ mice were incubated in lipid-deficient medium and treated with S2PNP-siCtrl or S2PNP-siEpsin1/2 for 48h, follow with treatment of 100 μg/mL oxLDL (A) or serum (B) collected from ApoE$^{-/-}$ mice fed a WD for 8 weeks. ORO staining was performed, scale bar=50μm.

Figure S18. S2PNP-siEpsin1/2 inhibits lesion formation and macrophage accumulation in early stage of atherosclerosis. (**A**) Male ApoE$^{-/-}$ mice were fed a WD for 8 weeks followed by treatment with S2PNP-siCtrl or S2PNP-siEpsin1/2 for 3 weeks (2 doses per week). (**B**) WB of Epsin 1 and 2 after treatment with S2PNP-siCtrl or S2PNP-siEpsin1/2 NPs using lesional lysates from the aortas (n=4 times). (**C-D**) Aortic roots from S2PNP-siCtrl treated ApoE$^{-/-}$ or S2PNP-siEpsin1/2 siRNA treated ApoE$^{-/-}$ mice were stained with the macrophage marker CD68 (solid white line) and Epsin1 or Epsin2 (dashed white line), Epsin 1 and 2 mean fluorescence intensity (MFI) were analyzed (n=5, scale bars=500 μm). (**E**) *En face* ORO staining of aortas (upper panel) and aortic root sections (lower panel) of hearts from baseline, S2PNP-siCtrl or S2PNP-siEpsin1/2 treated ApoE$^{-/-}$ mice fed a WD. Scale bar; aorta=5mm, aortic root=500μm.

Figure S19. Silencing lesional macrophage Epsin1/2 by S2PNP-siEpsin1/2 NP-treatment stabilized plaques in a progression model of atherosclerosis. ApoE$^{-/-}$ mice fed a WD for 17 weeks followed by treatment with S2PNP-siCtrl or S2PNP-siEpsin1/2 for 3 weeks (two doses per week). Van Gieson's staining of brachiocephalic artery (BCA) (upper panel) and aortic root (lower panel) sections from baseline, S2PNP-siCtrl-, or S2PNP-siEpsin1/2-treated ApoE$^{-/-}$ mice was performed (arrows indicate the elastic fibers, n=6, scale bar=250 μm).

Figure S20. Delivery of S2PNP-siEpsin1/2 does not change cholesterol and triglyceride levels of ApoE$^{-/-}$ mice fed a WD. Plasma from ApoE$^{-/-}$ mice fed a WD for 17 weeks (before NP injection), followed by an additional 3 weeks of treatment with S2PNP-siCtrl or S2PNP-siEspsin1/2, showed no alteration in triglyceride, cholesterol, HDL and non-HDL (LDL/VLDL) cholesterol levels (n=5).

Figure S21. Silencing macrophage Epsin1/2 by S2PNP-siEpsin1/2 NPs reduces lesion size in a regression model of atherosclerosis. (**A**) ORO staining of BCA sections in baseline, S2PNP-siCtrl or S2PNP-siEpsin1/2 treated PCSK9-mice was performed and lesions were indicated (dash

lines) (n=6, scale bar=500μm). (**B**) Van Gieson's staining of BCA sections from above three groups was performed (n=6, scale bar=500μm). (**C**) qRT-PCR analysis to confirm expression of the indicated genes (n=3).

Figure S22. S2PNP-siEpsin1/2 delivery inhibits the progression and regression of atherosclerosis in female mice. (**A**) Female ApoE$^{-/-}$ mice fed a Western Diet (WD) for 8 weeks followed by treatment of S2PNP-siCtrl or S2PNP-siEpsin1/2 for 3 weeks (2 doses per week). (**B**) Female ApoE$^{-/-}$ mice fed a Western Diet (WD) for 17 weeks followed by treatment of S2PNP-siCtrl or S2PNP-siEpsin1/2 for 3 weeks (2 doses per week, n=6mice per group). (**C**) Female C57BL/6 WT mice were injected twice with PCSK9-AAV8 (D377Y) virus and fed a WD for 16 weeks and followed by normal diet feeding with the treatment of S2PNP-siCtrl or S2PNP-siEpsin1/2 for 4 weeks (2 doses per week). (**D)** Statistic analysis of A. (**E)** Statistic analysis of B. (**F)** Statistic analysis of C. Scale bar: A, B, C=5mm.

Figure S23. Knockdown of Epsin1/2 in THP-1 macrophages show reduced lipid uptake, foam cell formation and increased cholesterol efflux to HDL. THP1 human monocytes-derived macrophages were differentiated with 10 ng/ml phorbol 12-myristate 13-acetate (PMA) for 48 hours and transfected with control siRNA and human epsin 1 and 2 siRNAs (2μg/each siRNA) for 24 hours. (**A**) Western blot was performed to confirm the knockdown of Epsin 1 and 2 in transfected THP1 macrophages. (**B**) Transfected THP1 macrophages were treated with 25μg/mL oxLDL for 24h in lipid-deficient medium. Oil Red O staining was performed to assess lipid accumulation and foam cell formation. (**C**) Transfected THP1 macrophages were incubated in lipid-deficient medium for 24h followed by the treatment with DiI-oxLDL for 2h at 37^0C to assess the lipid uptake. scale bar: B, C=50μm. (**D**) *In vitro* [^{3}H]-cholesterol labeled transfected THP1 macrophages were incubated in the presence or absence of HDL (25μg/mL) and ApoA-1 (10μg/mL) in the presence of 3μmol/L LXR agonist (T0901317) (n=9).

Figure S24. Epsins facilitates CD36-mediated lipid uptake and degradation of ABCG1 and LRP1 in THP1 macrophages. THP1 human monocytes-derived macrophages were differentiated with 10 ng/ml phorbol 12-myristate 13-acetate (PMA) for 48 hours and transfected with control siRNA and human epsin 1 and 2 siRNAs (2μg/each siRNA) for 24 hours. (**A-B**) Transfected THP1 macrophages were incubated in lipid-deficient medium for 24h and treated with or without 100μg/mL oxLDL for 45 min followed by staining with anti-CD36 (A) or anti-LRP1 (B) antibodies and analyzed by flow cytometry. (**C**) Transfected THP1 macrophages were treated with 3μmol/L liver X receptor (LXR) agonist in lipid-deficient medium for 24h, then treated with or without 100μg/mL oxLDL for 45 min followed by staining with Anti-ABCG1 antibody and analyzed by flow cytometry. (**E-G**) Statistic analysis for A-C, n=5 per group.

Figure S25. Summary schematic diagram of the study. (A) In the progression model of atherosclerosis, the plaque size and lesions increase in the artery on western diet feeding. The delivery of S2PNP-siEpsin1/2 significantly slowed the progression of atherosclerosis compared to S2PNP-siCtrl group. In the regression model of atherosclerosis, plaque size and lesion area were dramatically reduced with the intravenously injection of S2PNP-siEpsin1/2. (**B-C**). Under the stimuli of oxLDL, Epsin binds to CD36 and ABCG1 through Epsin ENTH and Epsin UIM domains, respectively. In B, Epsin facilitates CD36-mideated lipid uptake via recycling endosomes. The loss of Epsin impairs the internalization of CD36, which results in reduced lipid

uptake. While in C, Epsin promotes endocytic degradation of ABCG1via lysosomes, which leads to reduced total and surface level of ABCG1.

Supplemental Figures

Figure S1A

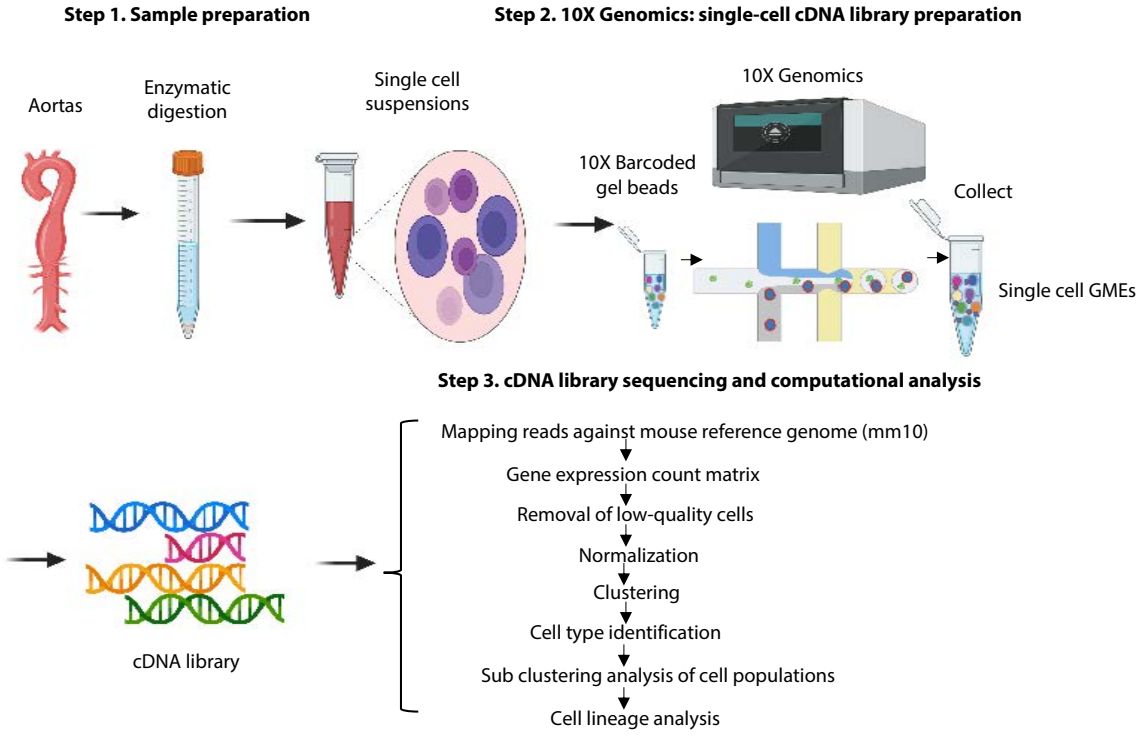

736 **Figure S1B**

737

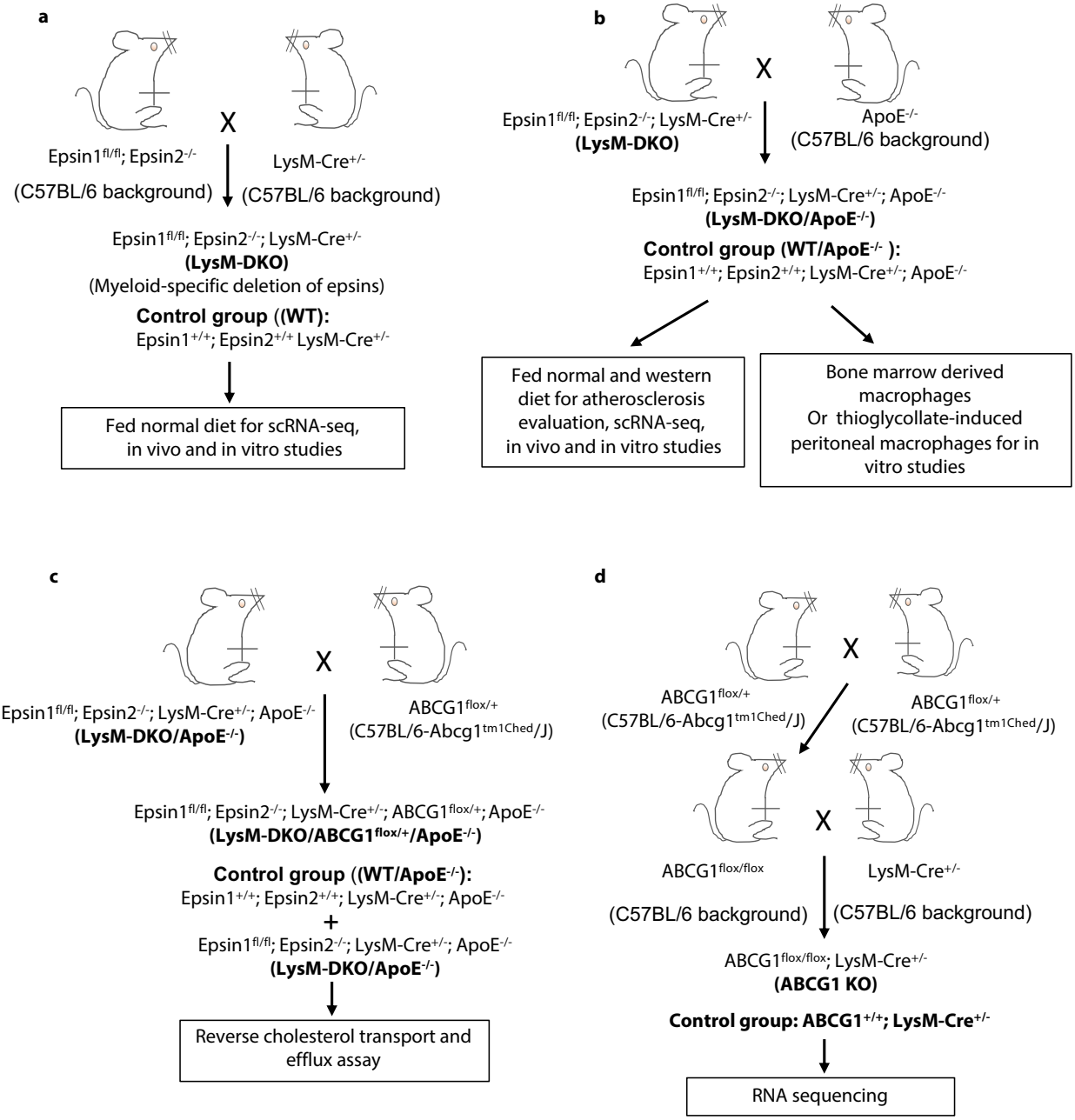

738

739

Figure S2

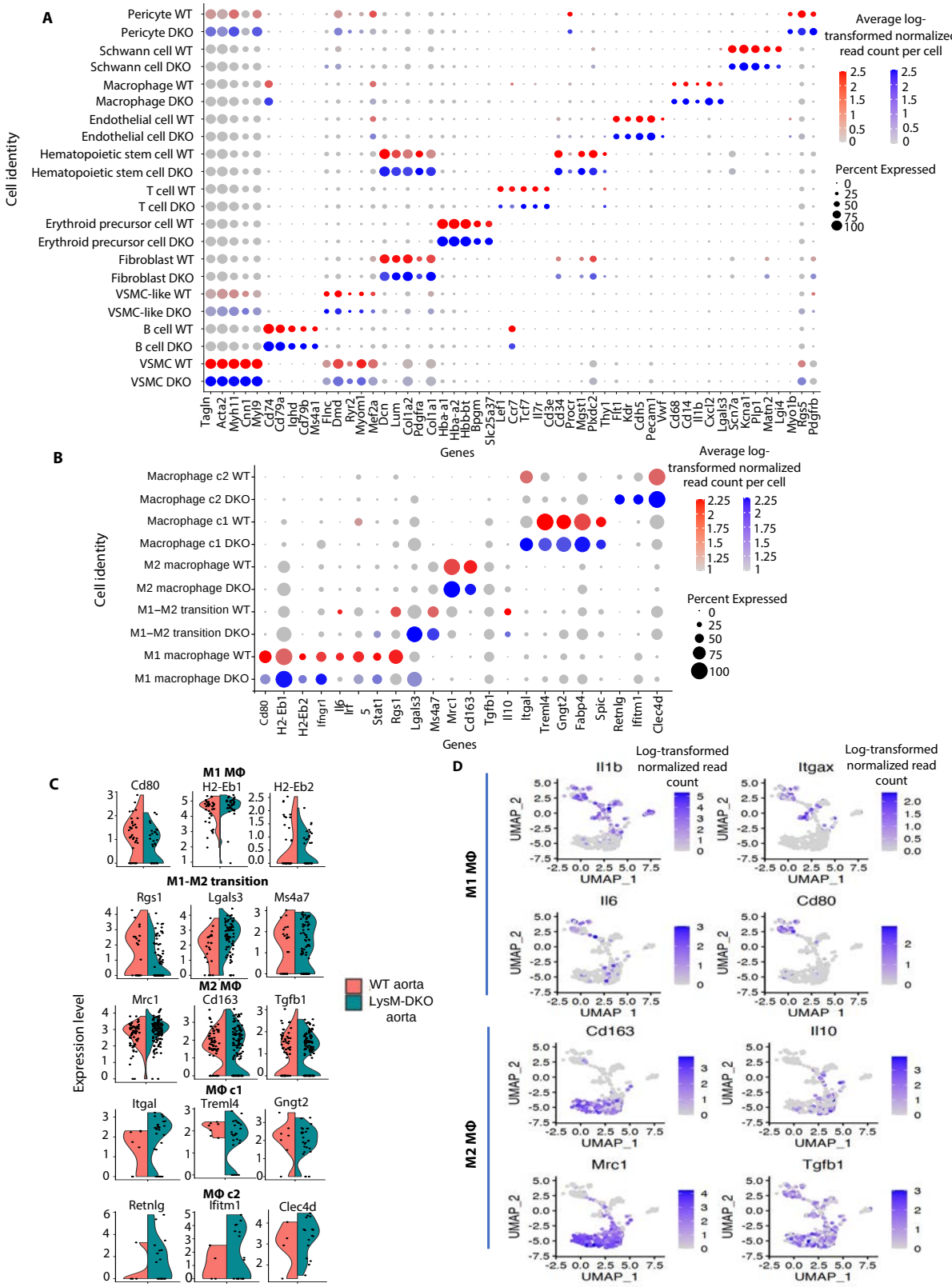
A
Cell identity
Pericyte WT
Pericyte DKO
Schwann cell WT
Schwann cell DKO
Macrophage WT
Macrophage DKO
Endothelial cell WT
Endothelial cell DKO
Hematopoietic stem cell WT
Hematopoietic stem cell DKO
T cell WT
T cell DKO
Erythroid precursor cell WT
Erythroid precursor cell DKO
Fibroblast WT
Fibroblast DKO
VSMC-like WT
VSMC-like DKO
B cell WT
B cell DKO
VSMC WT
VSMC DKO
Tagln Acta2 Myh11 Cnn1 Myl9 Cd74 Cd79a Ighd Cd79b Ms4a1 Flnc Dmd Ryr2 Myom1 Mef2a Dcn Lum Col1a2 Pdgfra Col1a1 Hba-a1 Hba-a2 Hbb-bt Bpgm Slc25a37 Lef1 Ccr7 Tcf7 Il7r Cd3e Cd34 Procr Mgst1 Pkdc2 Thy1 Flt1 Kdr Cdh5 Pecam1 Vwf Cd68 Cd14 Il1b Cxcl2 Lgals3 Scn7a Kcna1 Plp1 Matn2 Lgi4 Myo1b Rgs5 Pdgfrb
Genes
Average log-transformed normalized read count per cell
Percent Expressed
B
Cell identity
Macrophage c2 WT
Macrophage c2 DKO
Macrophage c1 WT
Macrophage c1 DKO
M2 macrophage WT
M2 macrophage DKO
M1–M2 transition WT
M1–M2 transition DKO
M1 macrophage WT
M1 macrophage DKO
Cd80 H2-Eb1 H2-Eb2 Ifngr1 Il6 Irf5 Stat1 Rgs1 Lgals3 Ms4a7 Mrc1 Cd163 Tgfb1 Il10 Itgal Treml4 Gngt2 Fabp4 Spic Retnlg Ifitm1 Clec4d
Genes
Average log-transformed normalized read count per cell
Percent Expressed
C
M1 MΦ
Cd80 H2-Eb1 H2-Eb2
M1-M2 transition
Rgs1 Lgals3 Ms4a7
M2 MΦ
Mrc1 Cd163 Tgfb1
MΦ c1
Itgal Treml4 Gngt2
MΦ c2
Retnlg Ifitm1 Clec4d
Expression level
WT aorta
LysM-DKO aorta
D
M1 MΦ
M2 MΦ
Il1b
Itgax
Il6
Cd80
Cd163
Il10
Mrc1
Tgfb1
UMAP_1
UMAP_2
Log-transformed normalized read count

Figure S3

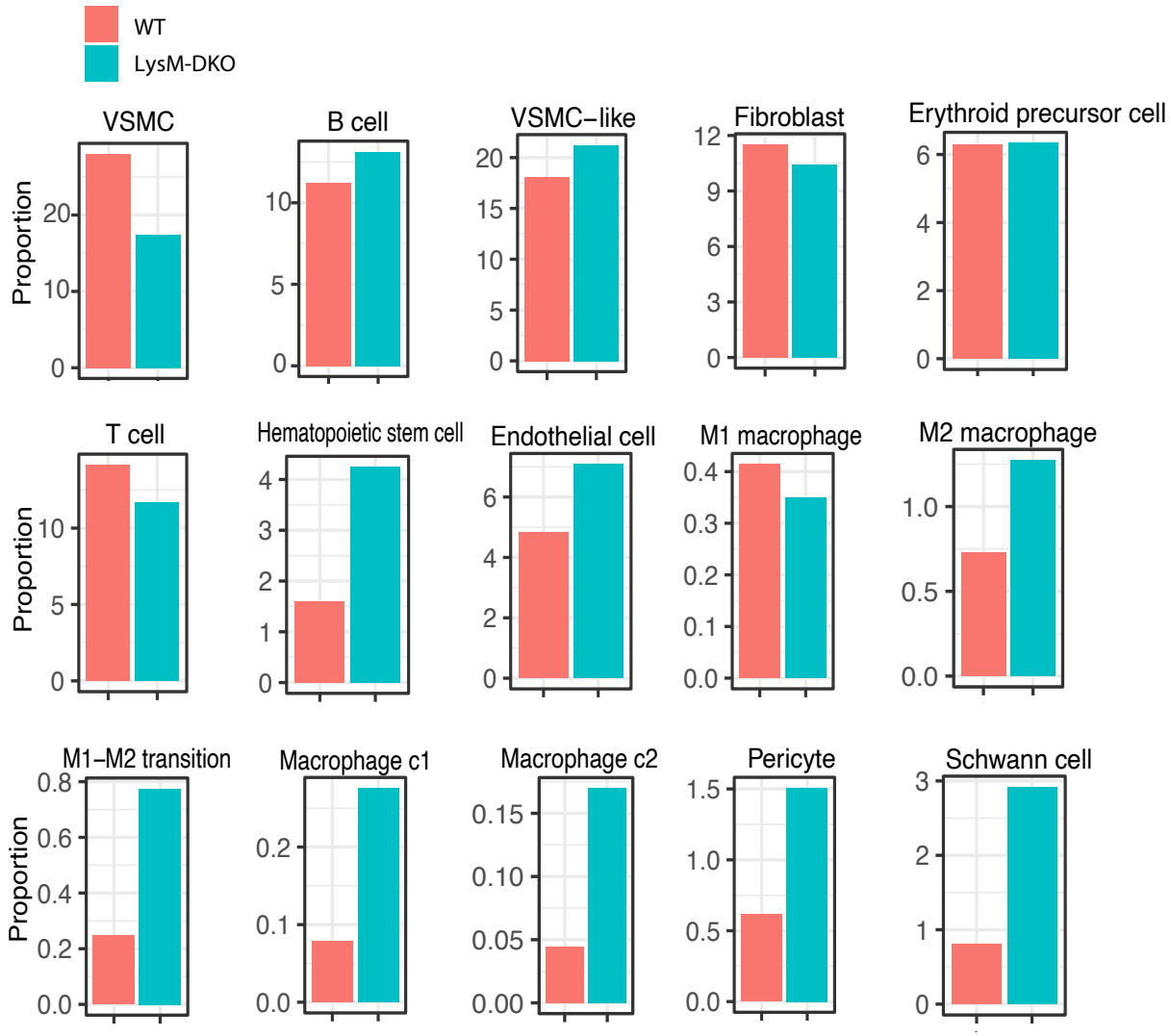
WT
LysM-DKO
VSMC
B cell
VSMC−like
Fibroblast
Erythroid precursor cell
T cell
Hematopoietic stem cell
Endothelial cell
M1 macrophage
M2 macrophage
M1−M2 transition
Macrophage c1
Macrophage c2
Pericyte
Schwann cell
Proportion

Figure S4

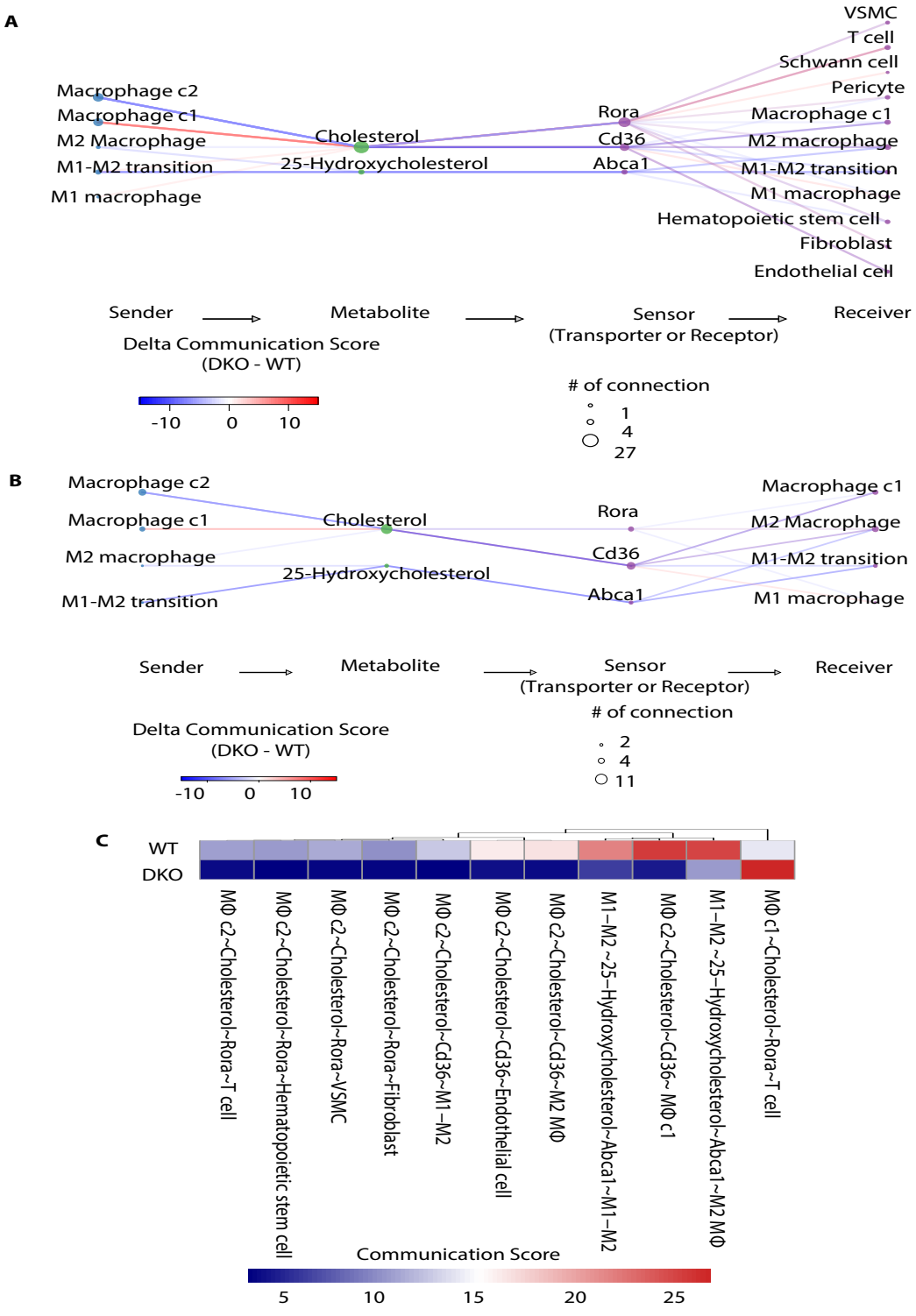
A
Macrophage c2
Macrophage c1
M2 Macrophage
M1-M2 transition
M1 macrophage
Cholesterol
25-Hydroxycholesterol
Rora
Cd36
Abca1
VSMC
T cell
Schwann cell
Pericyte
Macrophage c1
M2 macrophage
M1-M2 transition
M1 macrophage
Hematopoietic stem cell
Fibroblast
Endothelial cell
Sender
Metabolite
Sensor
(Transporter or Receptor)
Receiver
Delta Communication Score
(DKO - WT)
-10
0
10
# of connection
1
4
27
B
Macrophage c2
Macrophage c1
M2 macrophage
M1-M2 transition
Cholesterol
25-Hydroxycholesterol
Rora
Cd36
Abca1
Macrophage c1
M2 Macrophage
M1-M2 transition
M1 macrophage
Sender
Metabolite
Sensor
(Transporter or Receptor)
Receiver
Delta Communication Score
(DKO - WT)
-10
0
10
# of connection
2
4
11
C
WT
DKO
MΦ c2~Cholesterol~Rora~T cell
MΦ c2~Cholesterol~Rora~Hematopoietic stem cell
MΦ c2~Cholesterol~Rora~VSMC
MΦ c2~Cholesterol~Rora~Fibroblast
MΦ c2~Cholesterol~Cd36~M1−M2
MΦ c2~Cholesterol~Cd36~Endothelial cell
MΦ c2~Cholesterol~Cd36~M2 MΦ
M1−M2 ~25−Hydroxycholesterol~Abca1~M1−M2
MΦ c2~Cholesterol~Cd36~ MΦ c1
M1−M2 ~25−Hydroxycholesterol~Abca1~M2 MΦ
MΦ c1~Cholesterol~Rora~T cell
Communication Score
5
10
15
20
25

751 **Figure S5**

752

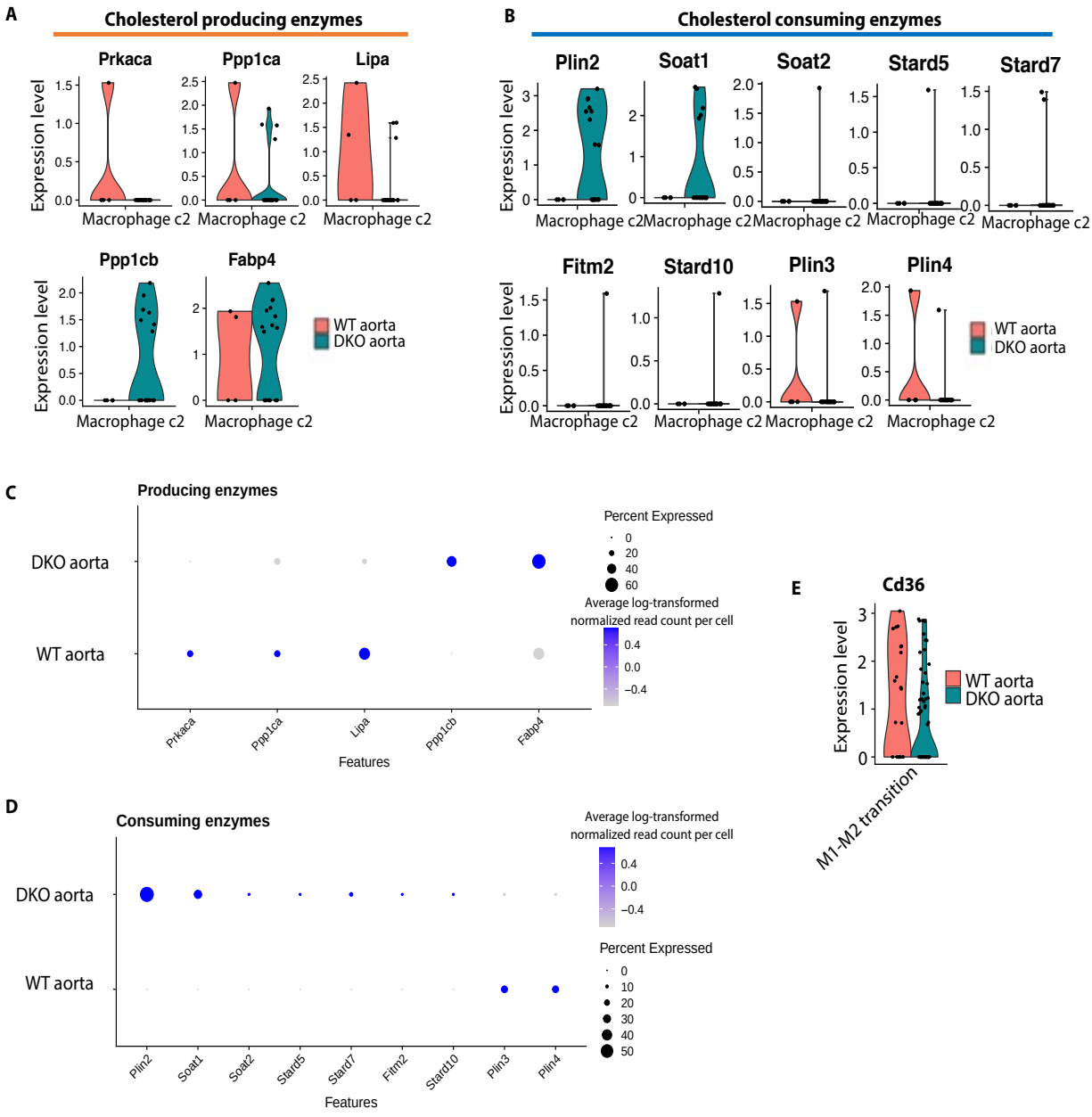

753

Figure S6

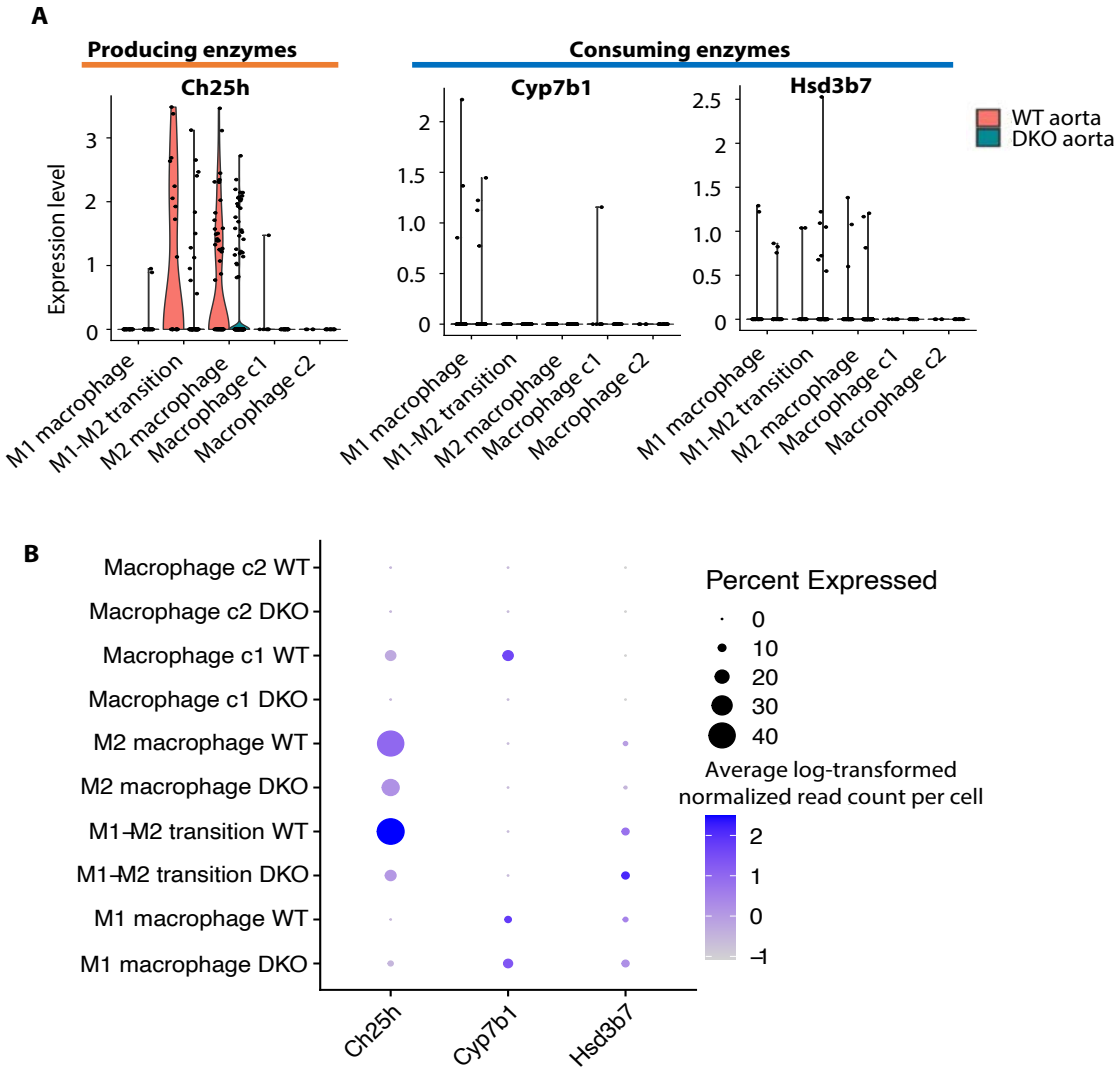
A
Producing enzymes
Consuming enzymes
Ch25h
Cyp7b1
Hsd3b7
Expression level
WT aorta
DKO aorta
M1 macrophage
M1-M2 transition
M2 macrophage
Macrophage c1
Macrophage c2
B
Macrophage c2 WT
Macrophage c2 DKO
Macrophage c1 WT
Macrophage c1 DKO
M2 macrophage WT
M2 macrophage DKO
M1-M2 transition WT
M1-M2 transition DKO
M1 macrophage WT
M1 macrophage DKO
Ch25h
Cyp7b1
Hsd3b7
Percent Expressed
Average log-transformed normalized read count per cell

Figure S7

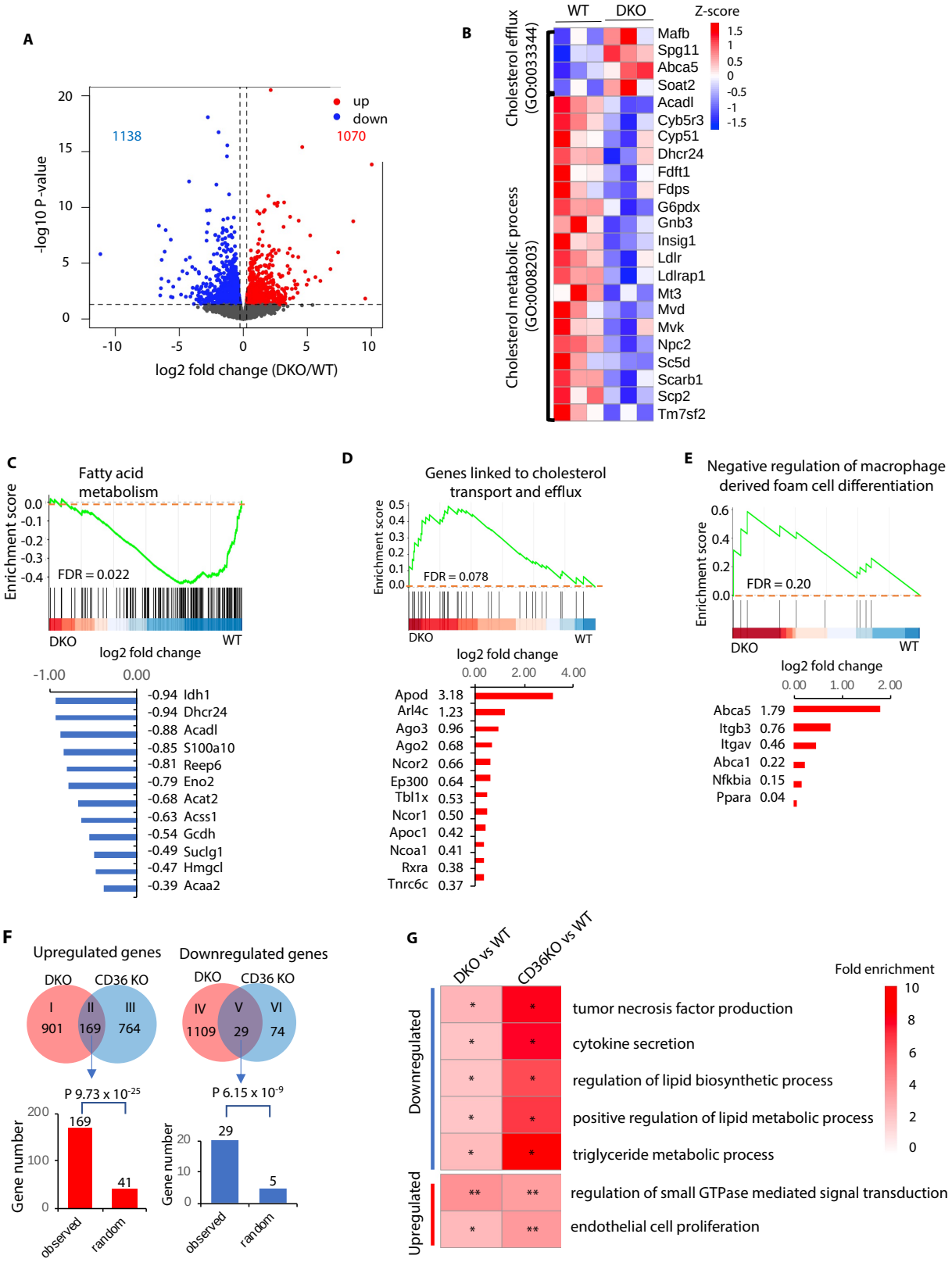
A
up
down
1138
1070
-log10 P-value
log2 fold change (DKO/WT)
B
WT
DKO
Z-score
Cholesterol efflux (GO:0033344)
Cholesterol metabolic process (GO:0008203)
Mafb
Spg11
Abca5
Soat2
Acadl
Cyb5r3
Cyp51
Dhcr24
Fdft1
Fdps
G6pdx
Gnb3
Insig1
Ldlr
Ldlrap1
Mt3
Mvd
Mvk
Npc2
Sc5d
Scarb1
Scp2
Tm7sf2
C
Fatty acid metabolism
Enrichment score
FDR = 0.022
DKO
WT
log2 fold change
-0.94 Idh1
-0.94 Dhcr24
-0.88 Acadl
-0.85 S100a10
-0.81 Reep6
-0.79 Eno2
-0.68 Acat2
-0.63 Acss1
-0.54 Gcdh
-0.49 Suclg1
-0.47 Hmgcl
-0.39 Acaa2
D
Genes linked to cholesterol transport and efflux
FDR = 0.078
Apod 3.18
Arl4c 1.23
Ago3 0.96
Ago2 0.68
Ncor2 0.66
Ep300 0.64
Tbl1x 0.53
Ncor1 0.50
Apoc1 0.42
Ncoa1 0.41
Rxra 0.38
Tnrc6c 0.37
E
Negative regulation of macrophage derived foam cell differentiation
FDR = 0.20
Abca5 1.79
Itgb3 0.76
Itgav 0.46
Abca1 0.22
Nfkbia 0.15
Ppara 0.04
F
Upregulated genes
Downregulated genes
DKO
CD36 KO
I 901
II 169
III 764
IV 1109
V 29
VI 74
P 9.73 x 10-25
P 6.15 x 10-9
Gene number
observed
random
G
DKO vs WT
CD36KO vs WT
Fold enrichment
Downregulated
Upregulated
tumor necrosis factor production
cytokine secretion
regulation of lipid biosynthetic process
positive regulation of lipid metabolic process
triglyceride metabolic process
regulation of small GTPase mediated signal transduction
endothelial cell proliferation

761 **Figure S8**
762

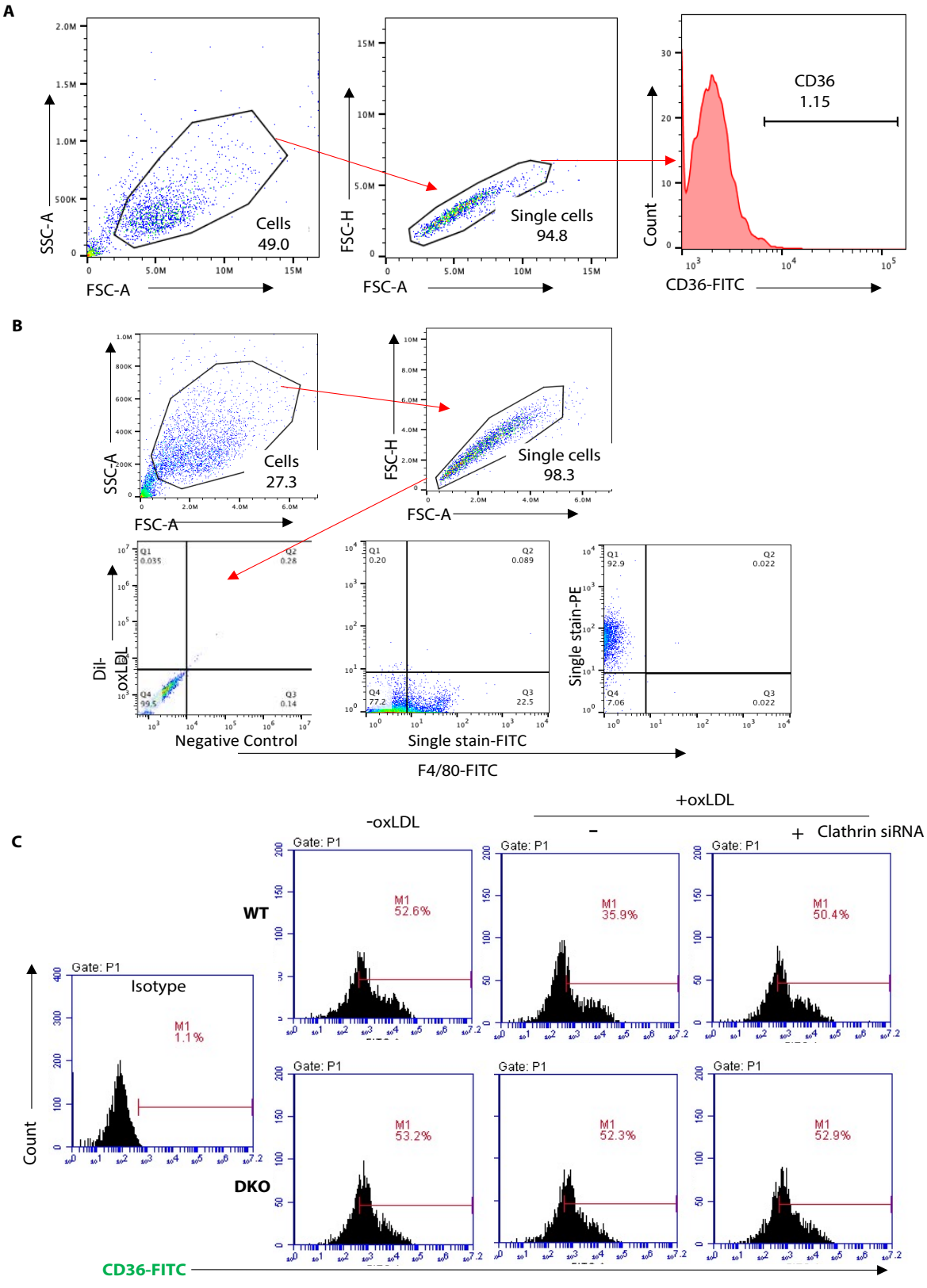

763

Figure S9

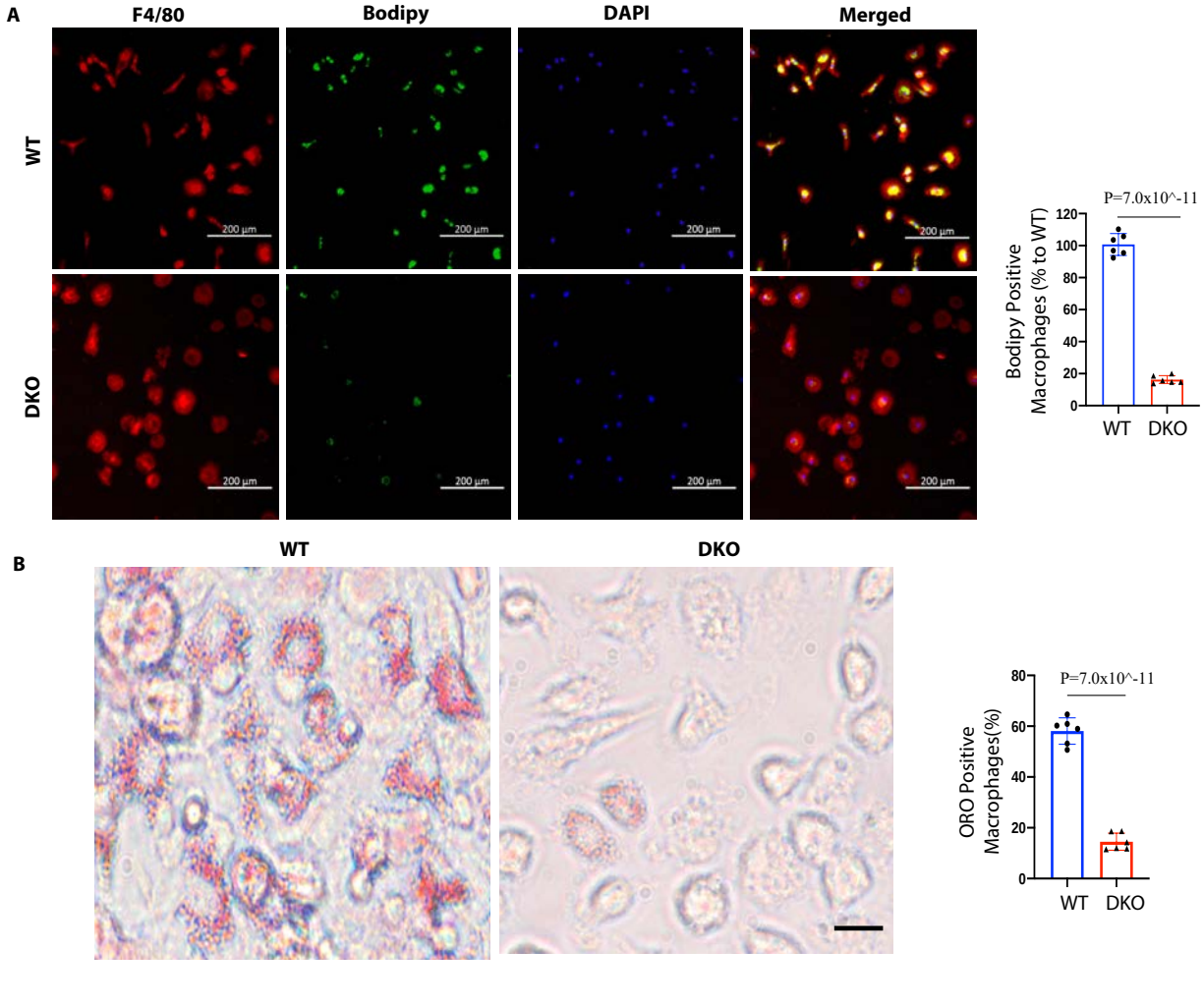
A
F4/80
Bodipy
DAPI
Merged
WT
DKO
200 µm
Bodipy Positive Macrophages (% to WT)
P=7.0x10^-11
120
100
80
60
40
20
0
WT
DKO
B
WT
DKO
ORO Positive Macrophages(%)
P=7.0x10^-11
80
60
40
20
0
WT
DKO

769 **Figure S10**
770
771

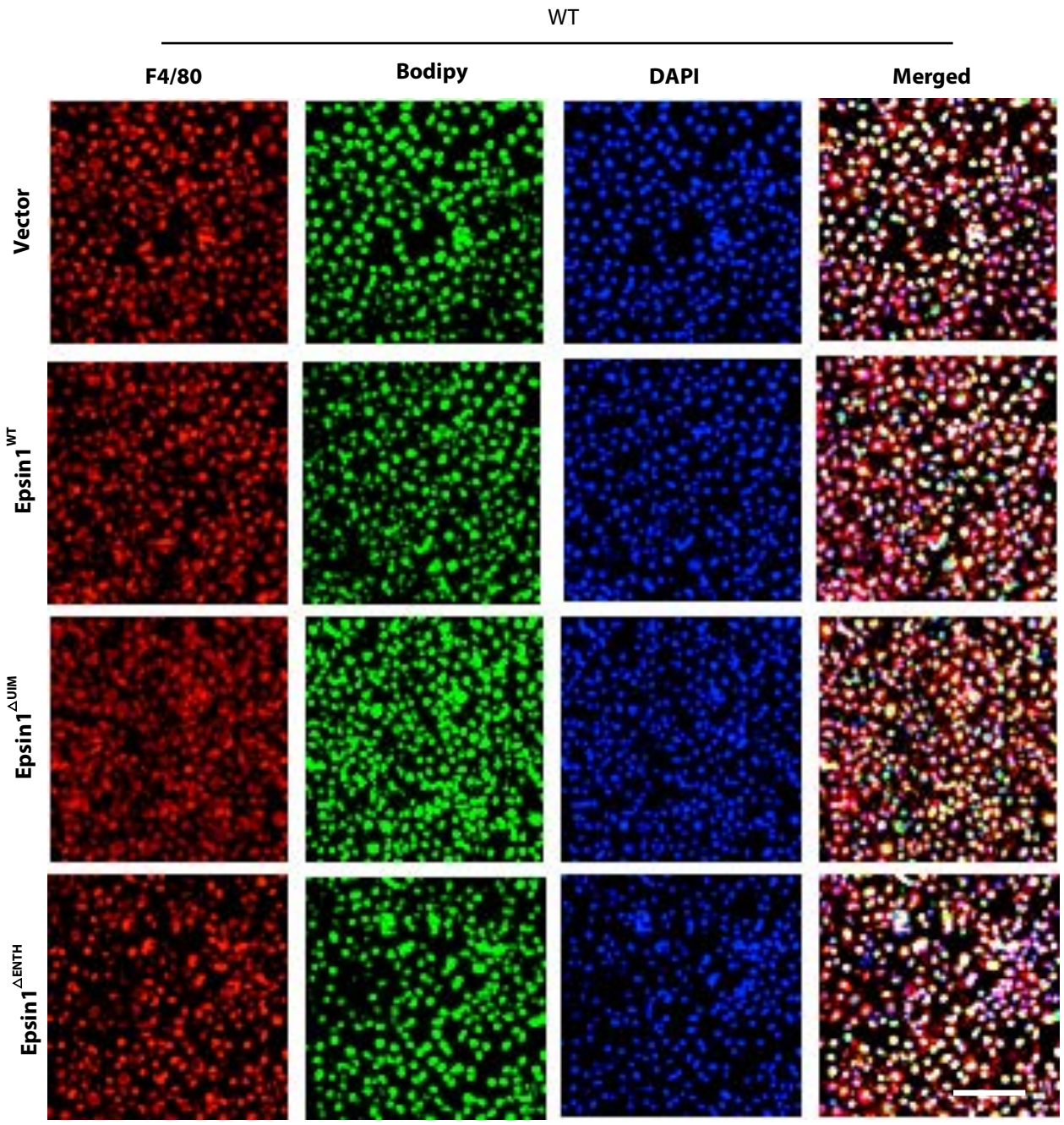

Figure S11

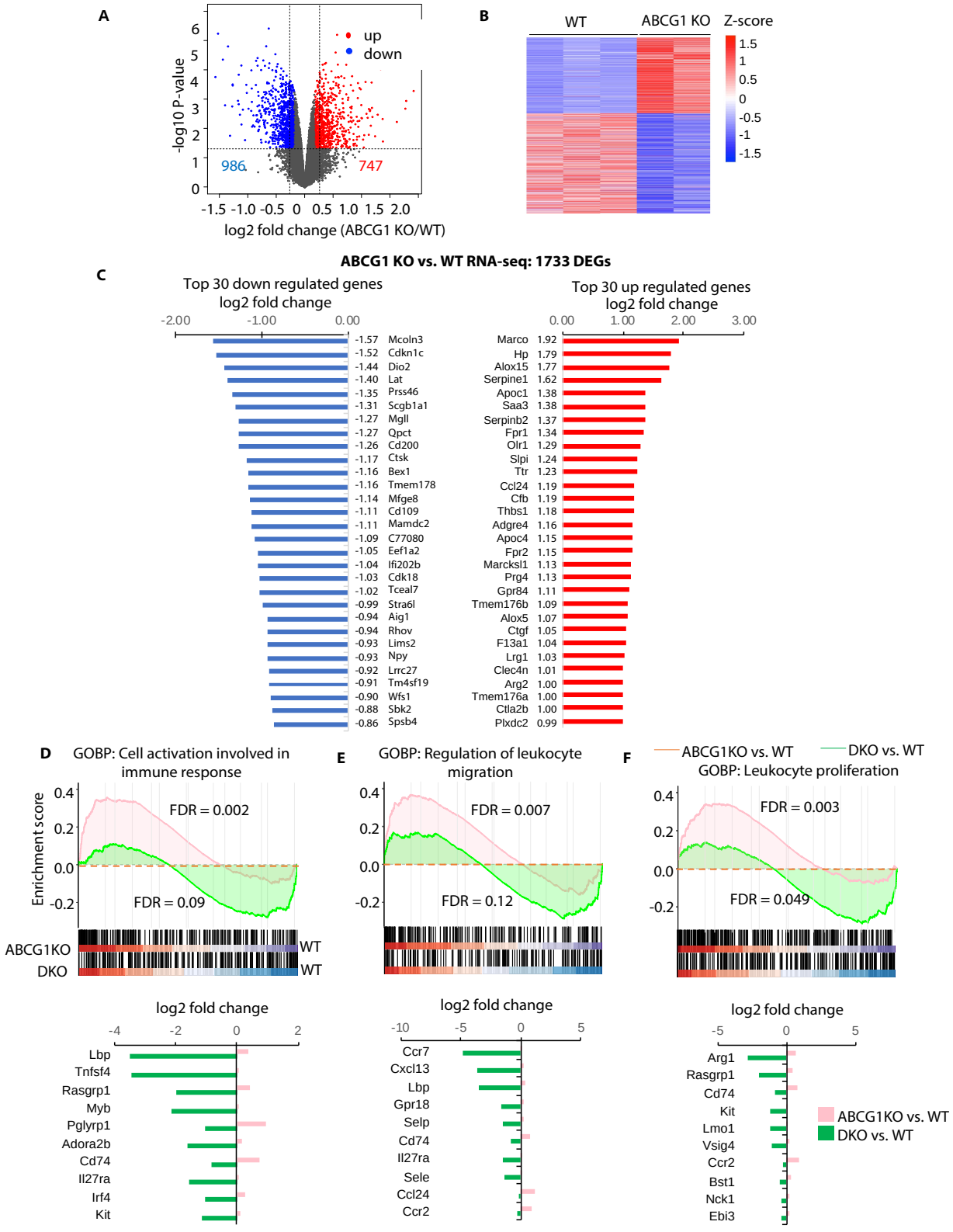
A
up
down
-log10 P-value
986
747
log2 fold change (ABCG1 KO/WT)
B
WT
ABCG1 KO
Z-score
C
ABCG1 KO vs. WT RNA-seq: 1733 DEGs
Top 30 down regulated genes
log2 fold change
Top 30 up regulated genes
log2 fold change
D
GOBP: Cell activation involved in immune response
FDR = 0.002
FDR = 0.09
Enrichment score
ABCG1KO
DKO
WT
WT
log2 fold change
E
GOBP: Regulation of leukocyte migration
FDR = 0.007
FDR = 0.12
log2 fold change
F
ABCG1KO vs. WT
DKO vs. WT
GOBP: Leukocyte proliferation
FDR = 0.003
FDR = 0.049
log2 fold change
ABCG1KO vs. WT
DKO vs. WT

Figure S12

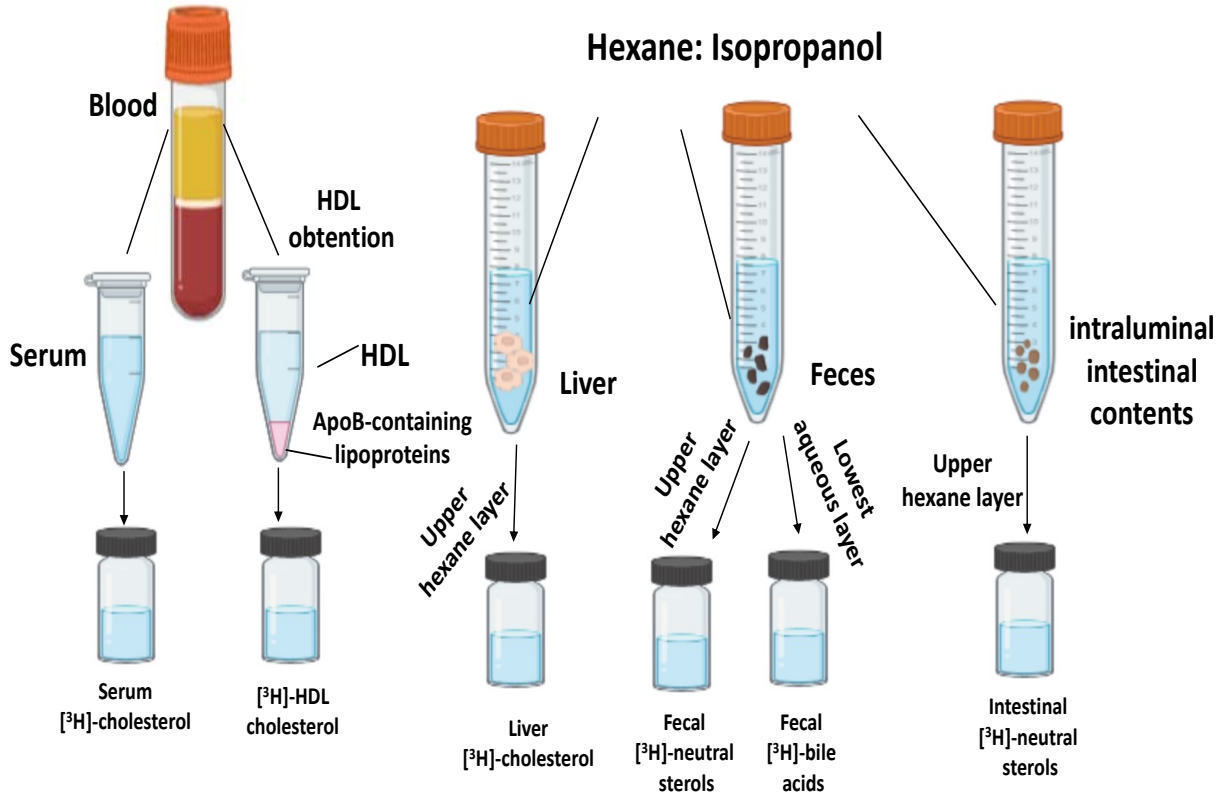

Figure S13

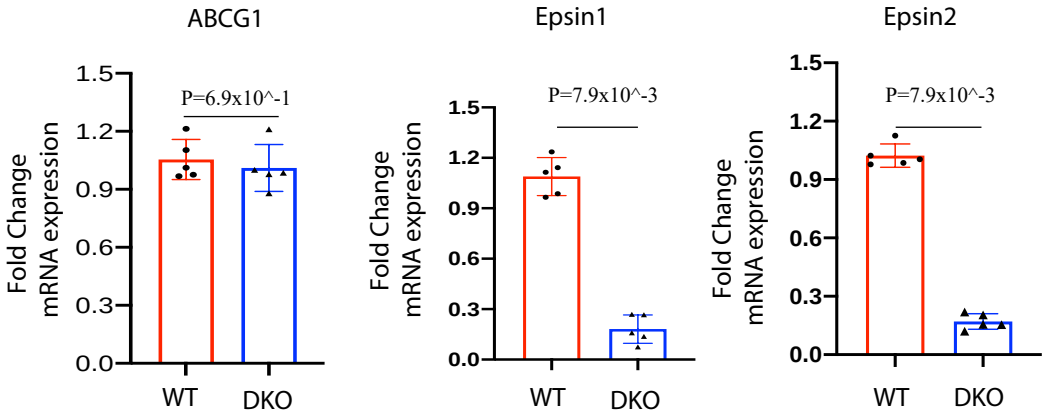

Figure S14

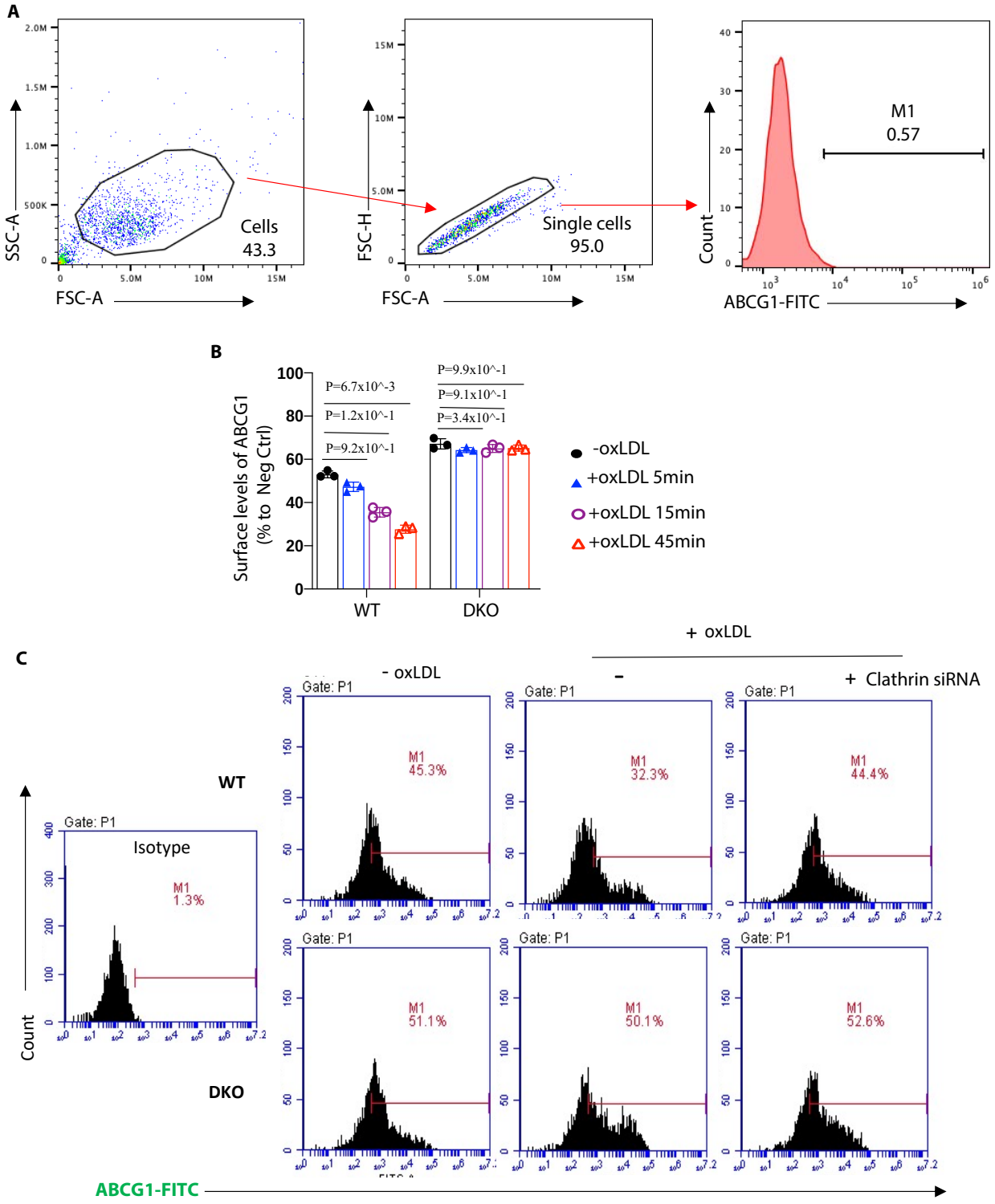
A
SSC-A
FSC-A
Cells
43.3
FSC-H
FSC-A
Single cells
95.0
Count
ABCG1-FITC
M1
0.57
B
Surface levels of ABCG1
(% to Neg Ctrl)
P=6.7x10^-3
P=1.2x10^-1
P=9.2x10^-1
P=9.9x10^-1
P=9.1x10^-1
P=3.4x10^-1
WT
DKO
-oxLDL
+oxLDL 5min
+oxLDL 15min
+oxLDL 45min
C
+ oxLDL
- oxLDL
-
+ Clathrin siRNA
WT
DKO
Gate: P1
Isotype
M1
1.3%
M1
45.3%
M1
32.3%
M1
44.4%
M1
51.1%
M1
50.1%
M1
52.6%
Count
ABCG1-FITC

Figure S15

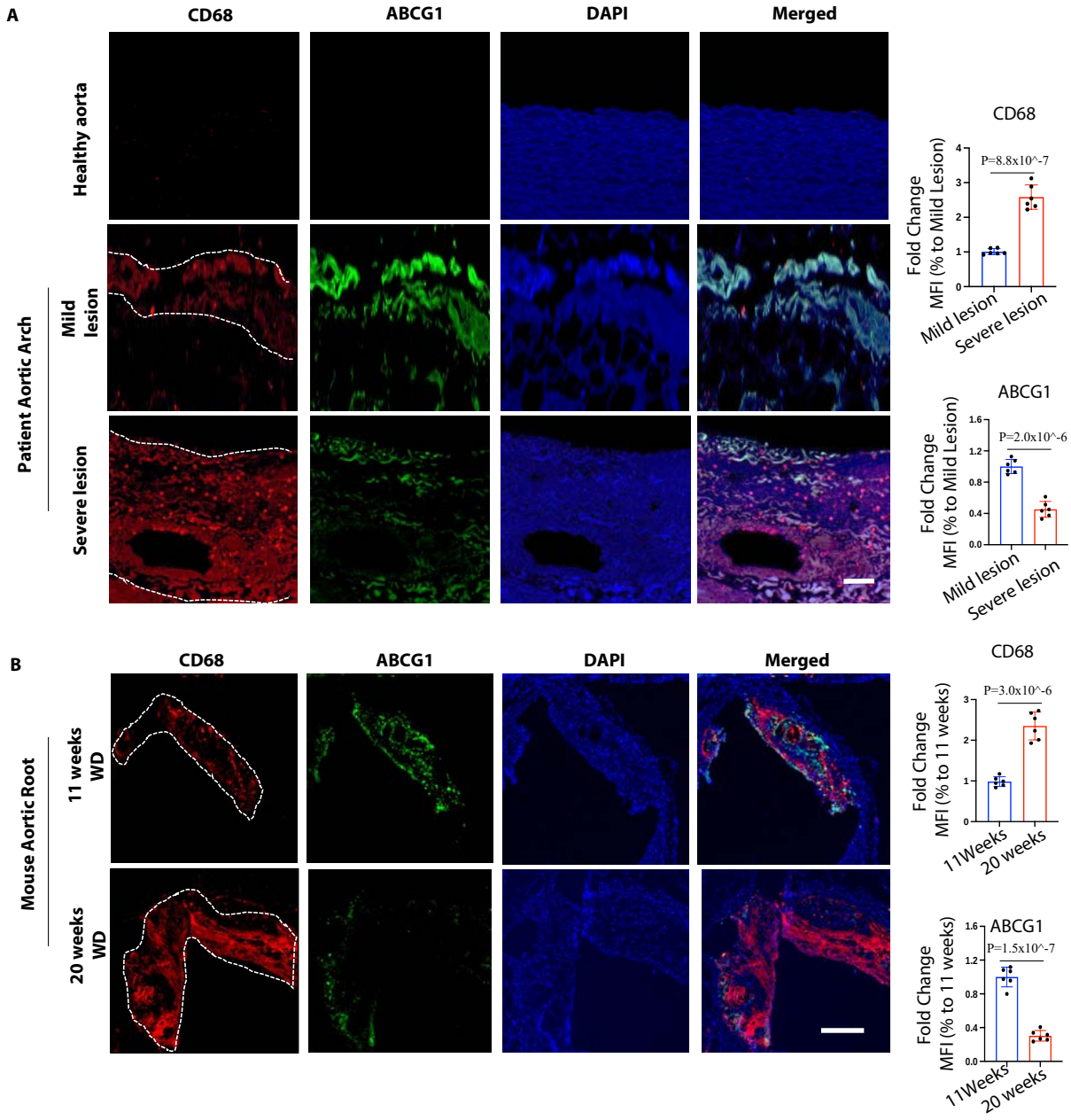
A
CD68
ABCG1
DAPI
Merged
Healthy aorta
Patient Aortic Arch
Mild lesion
Severe lesion
CD68
Fold Change MFI (% to Mild Lesion)
P=8.8x10^-7
Mild lesion
Severe lesion
ABCG1
Fold Change MFI (% to Mild Lesion)
P=2.0x10^-6
Mild lesion
Severe lesion
B
CD68
ABCG1
DAPI
Merged
Mouse Aortic Root
11 weeks WD
20 weeks WD
CD68
Fold Change MFI (% to 11 weeks)
P=3.0x10^-6
11Weeks
20 weeks
ABCG1
Fold Change MFI (% to 11 weeks)
P=1.5x10^-7
11Weeks
20 weeks

797 **Figure S16**
798
799

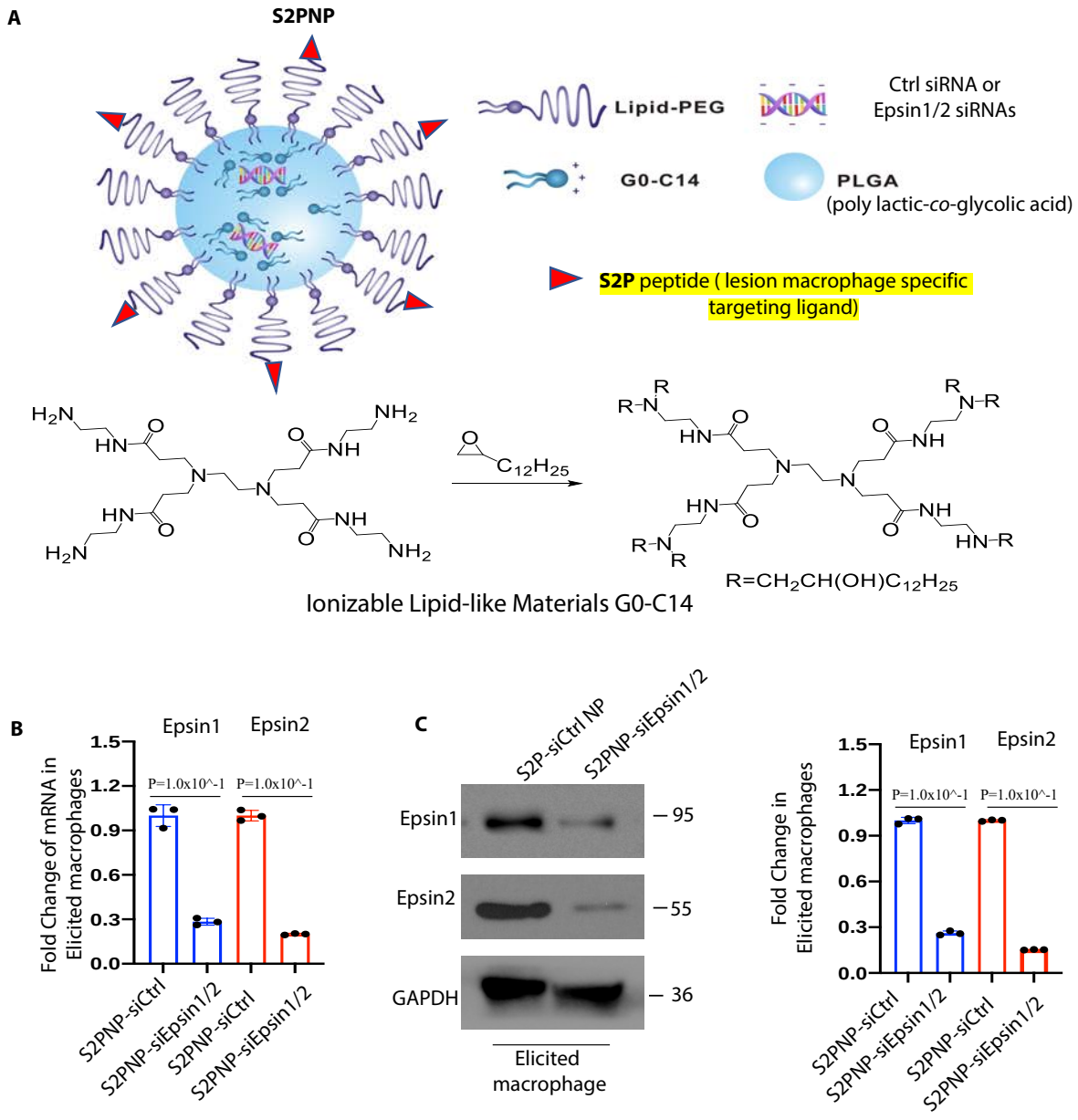

800

Figure S17

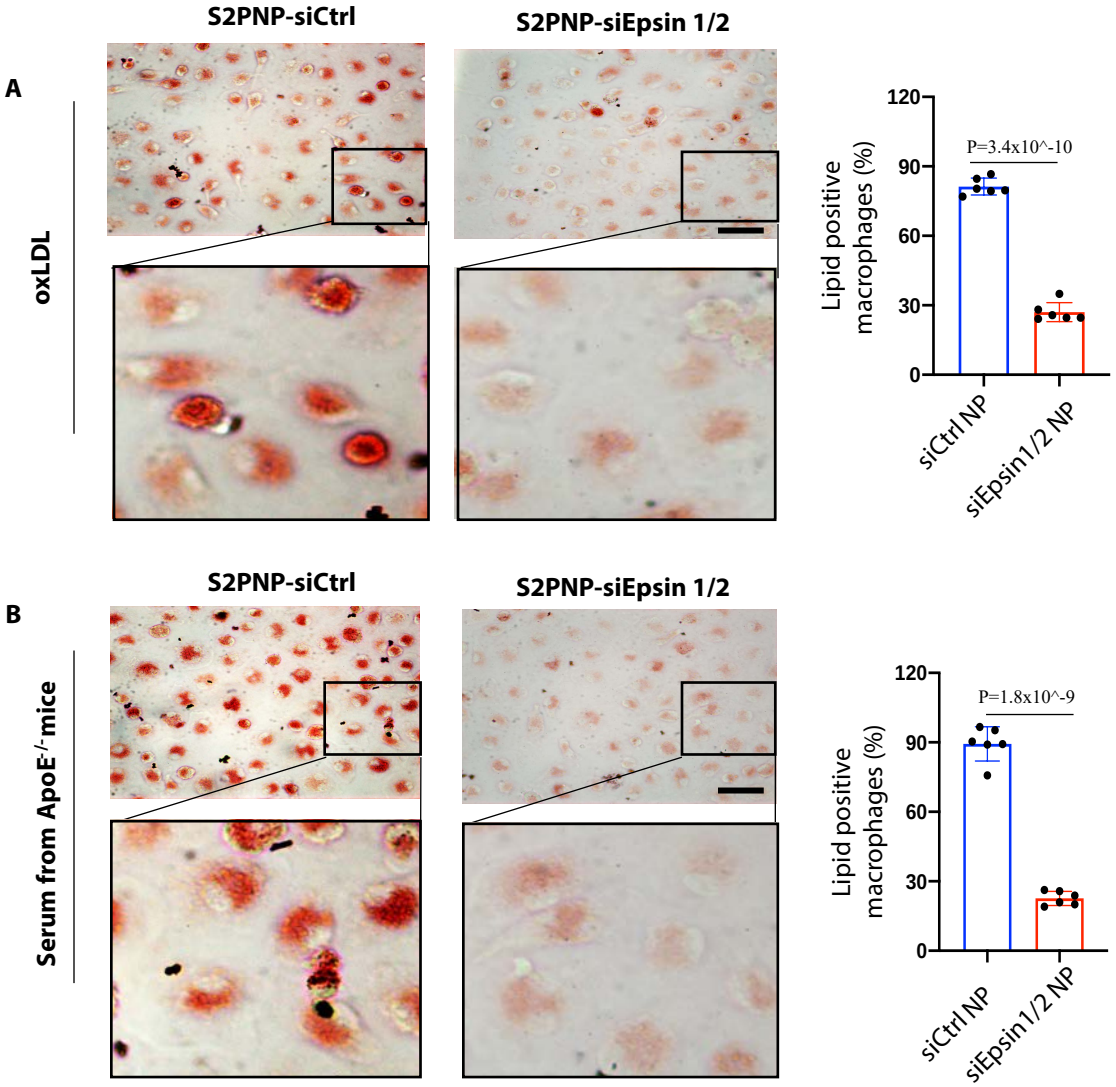
S2PNP-siCtrl
S2PNP-siEpsin 1/2
A
oxLDL
Lipid positive macrophages (%)
P=3.4x10^-10
120
90
60
30
0
siCtrl NP
siEpsin1/2 NP
S2PNP-siCtrl
S2PNP-siEpsin 1/2
B
Serum from ApoE-/- mice
Lipid positive macrophages (%)
P=1.8x10^-9
120
90
60
30
0
siCtrl NP
siEpsin1/2 NP

Figure S18

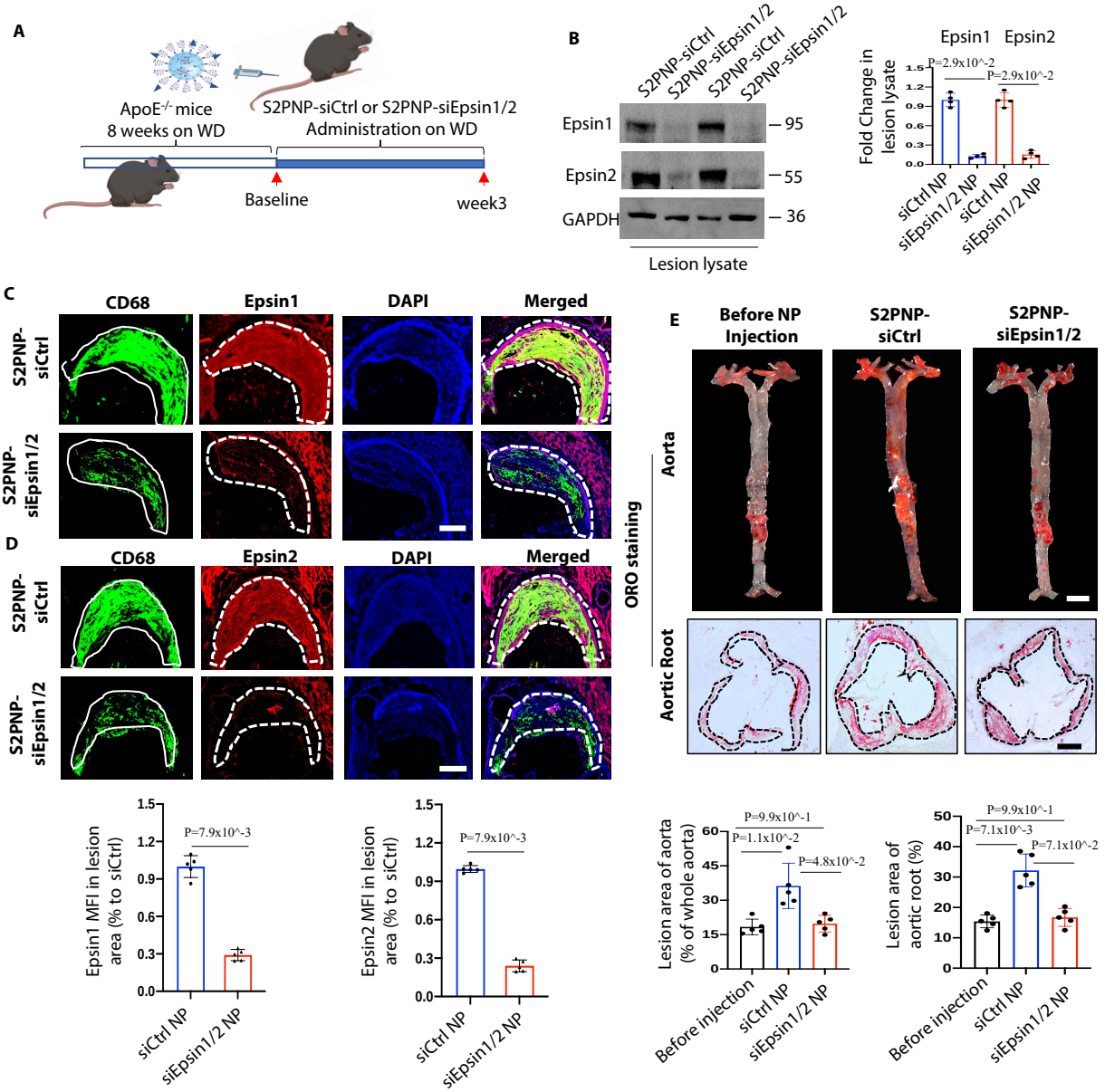
A
ApoE-/- mice
8 weeks on WD
S2PNP-siCtrl or S2PNP-siEpsin1/2
Administration on WD
Baseline
week3
B
S2PNP-siCtrl
S2PNP-siEpsin1/2
S2PNP-siCtrl
S2PNP-siEpsin1/2
Epsin1
Epsin2
GAPDH
95
55
36
Lesion lysate
Epsin1 Epsin2
Fold Change in lesion lysate
P=2.9x10^-2
P=2.9x10^-2
siCtrl NP
siEpsin1/2 NP
siCtrl NP
siEpsin1/2 NP
C
CD68
Epsin1
DAPI
Merged
S2PNP-siCtrl
S2PNP-siEpsin1/2
D
CD68
Epsin2
DAPI
Merged
S2PNP-siCtrl
S2PNP-siEpsin1/2
E
Before NP Injection
S2PNP-siCtrl
S2PNP-siEpsin1/2
ORO staining
Aorta
Aortic Root
Epsin1 MFI in lesion area (% to siCtrl)
P=7.9x10^-3
siCtrl NP
siEpsin1/2 NP
Epsin2 MFI in lesion area (% to siCtrl)
P=7.9x10^-3
siCtrl NP
siEpsin1/2 NP
Lesion area of aorta (% of whole aorta)
P=9.9x10^-1
P=1.1x10^-2
P=4.8x10^-2
Before injection
siCtrl NP
siEpsin1/2 NP
Lesion area of aortic root (%)
P=9.9x10^-1
P=7.1x10^-3
P=7.1x10^-2
Before injection
siCtrl NP
siEpsin1/2 NP

Figure S19

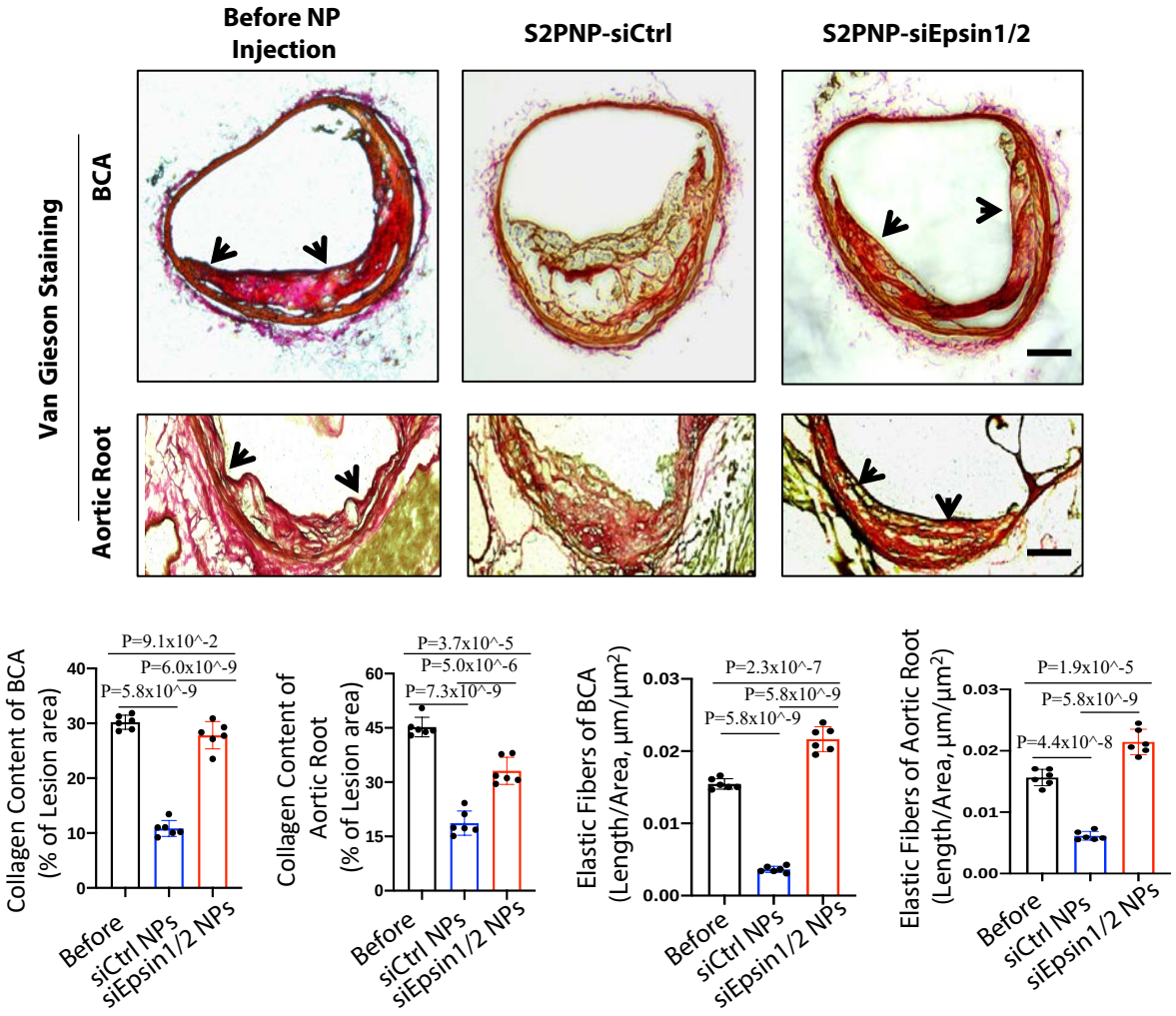

Figure S20

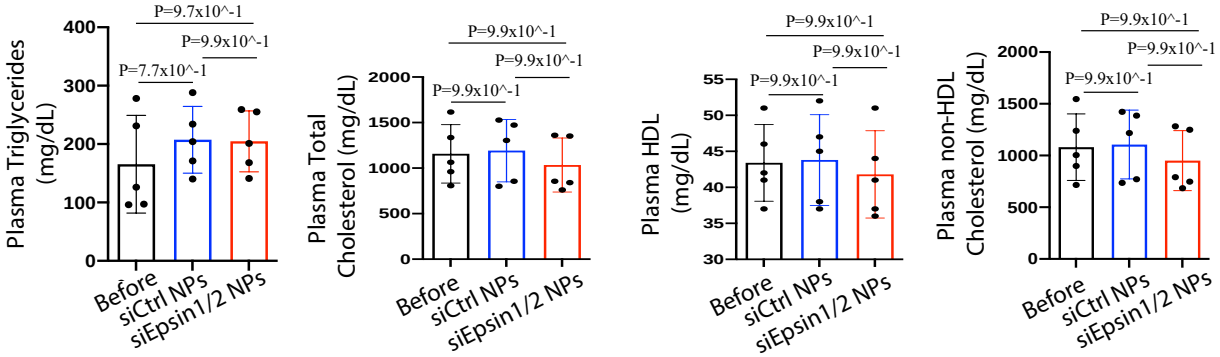

819 **Figure S21**

820

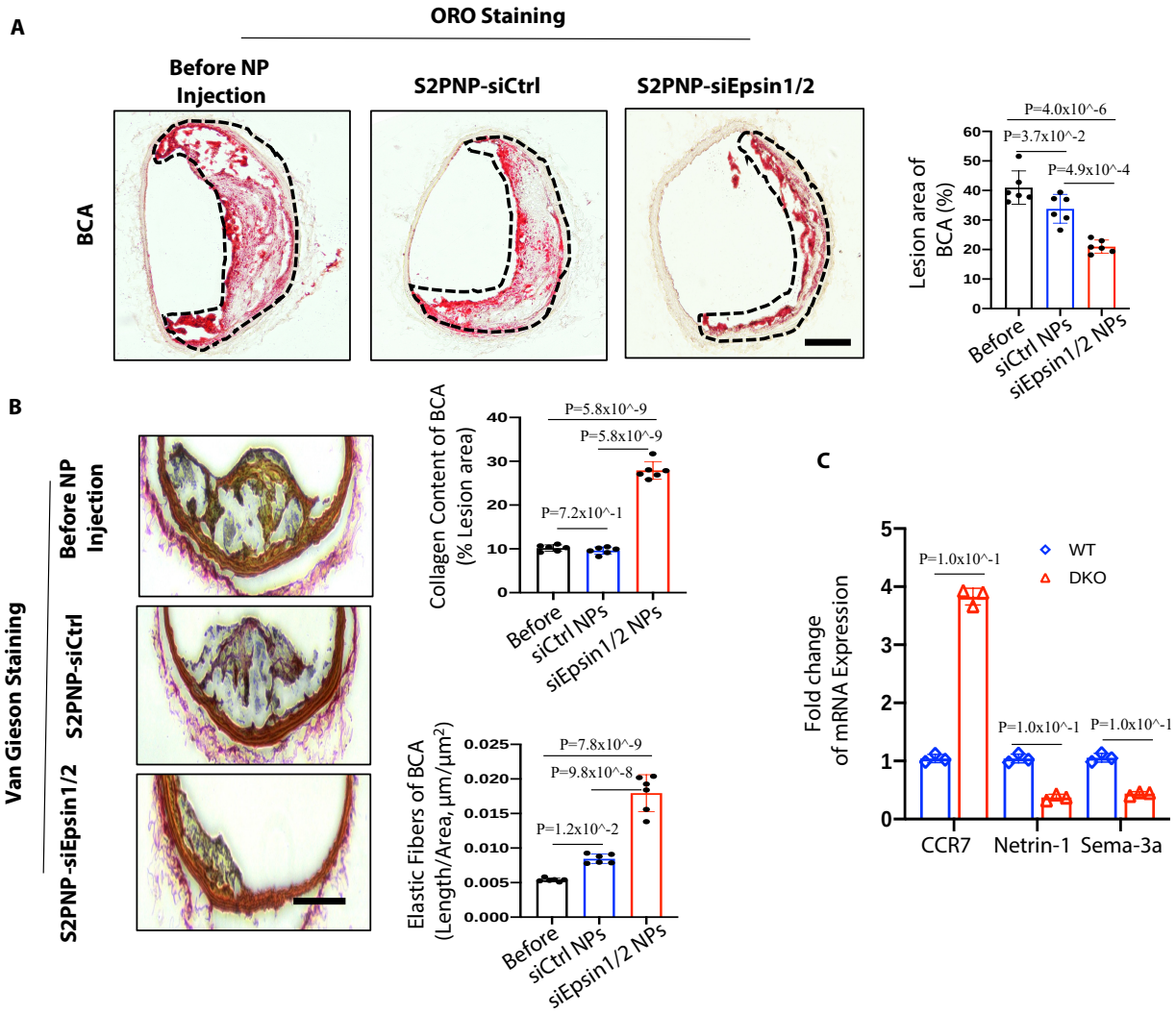

821

822 **Figure S22**

823

824

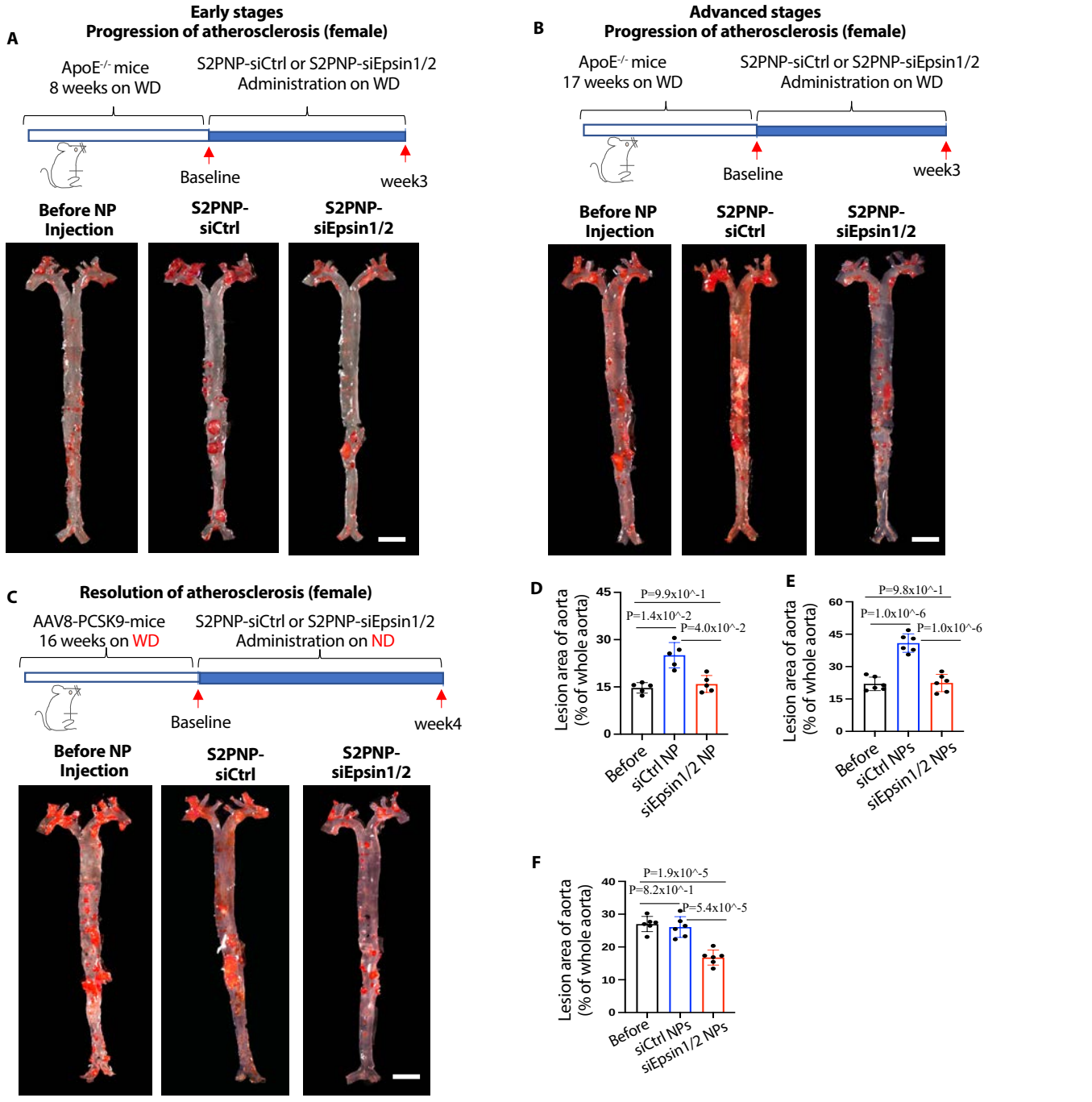

825

826

827

828 **Figure S23**
829
830

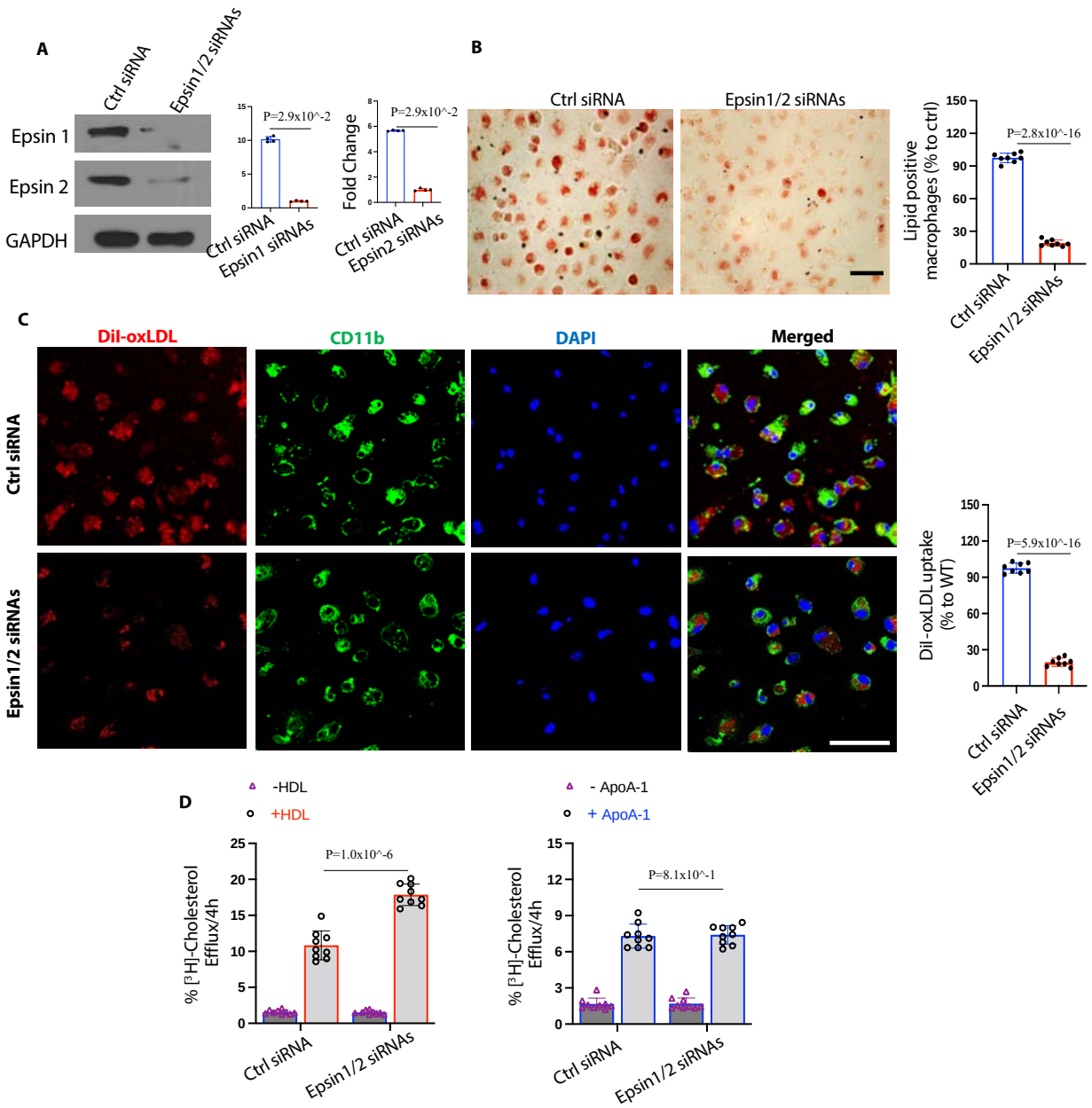

831
832

Figure S24

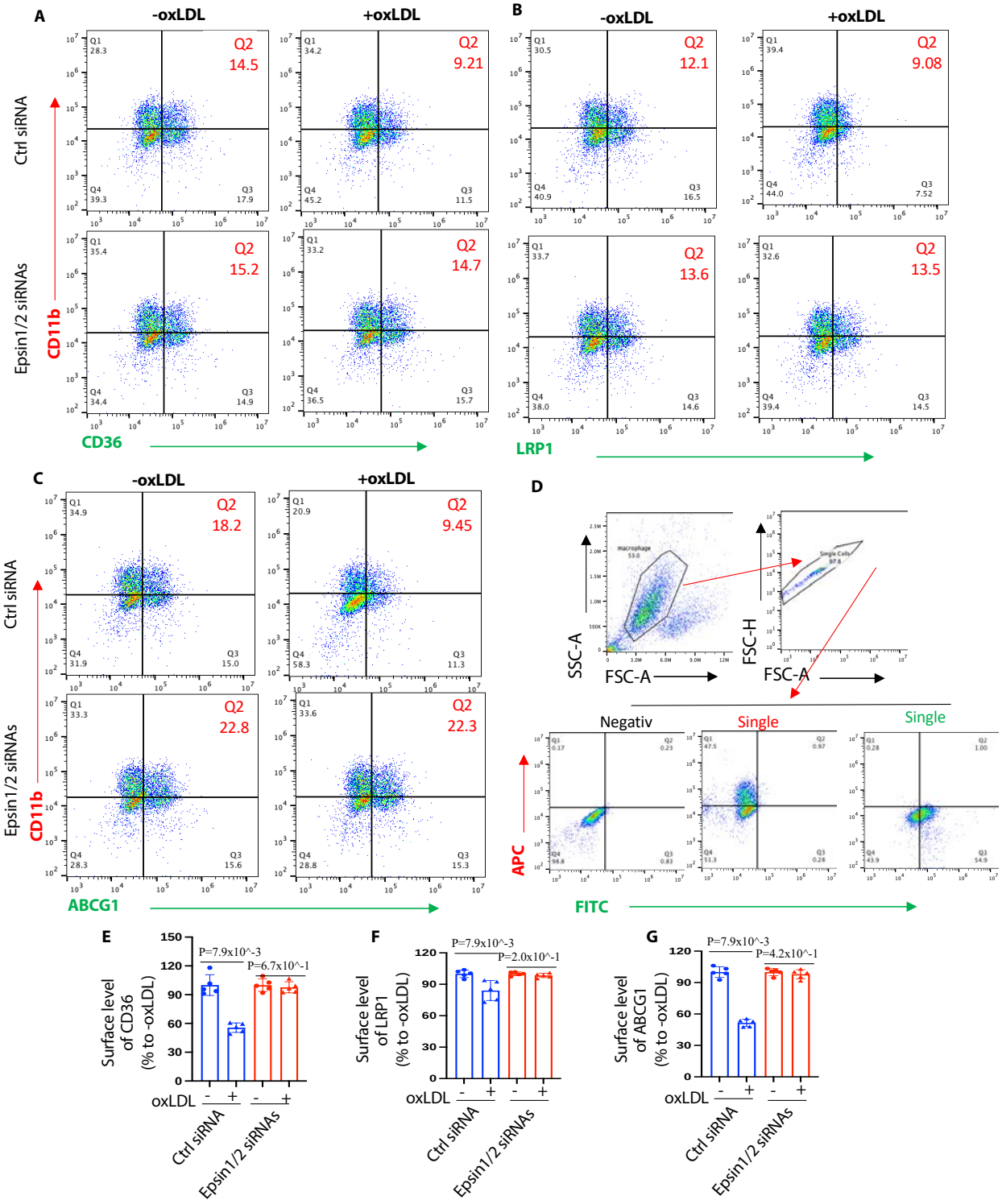
A
-oxLDL
+oxLDL
Ctrl siRNA
Epsin1/2 siRNAs
CD11b
CD36
Q2 14.5
Q2 9.21
Q2 15.2
Q2 14.7
B
-oxLDL
+oxLDL
LRP1
Q2 12.1
Q2 9.08
Q2 13.6
Q2 13.5
C
-oxLDL
+oxLDL
ABCG1
Q2 18.2
Q2 9.45
Q2 22.8
Q2 22.3
D
SSC-A
FSC-A
FSC-H
FSC-A
Negativ
Single
Single
APC
FITC
E
Surface level of CD36 (% to -oxLDL)
P=7.9x10^-3
P=6.7x10^-1
oxLDL
Ctrl siRNA
Epsin1/2 siRNAs
F
Surface level of LRP1 (% to -oxLDL)
P=7.9x10^-3
P=2.0x10^-1
G
Surface level of ABCG1 (% to -oxLDL)
P=7.9x10^-3
P=4.2x10^-1

Figure S25

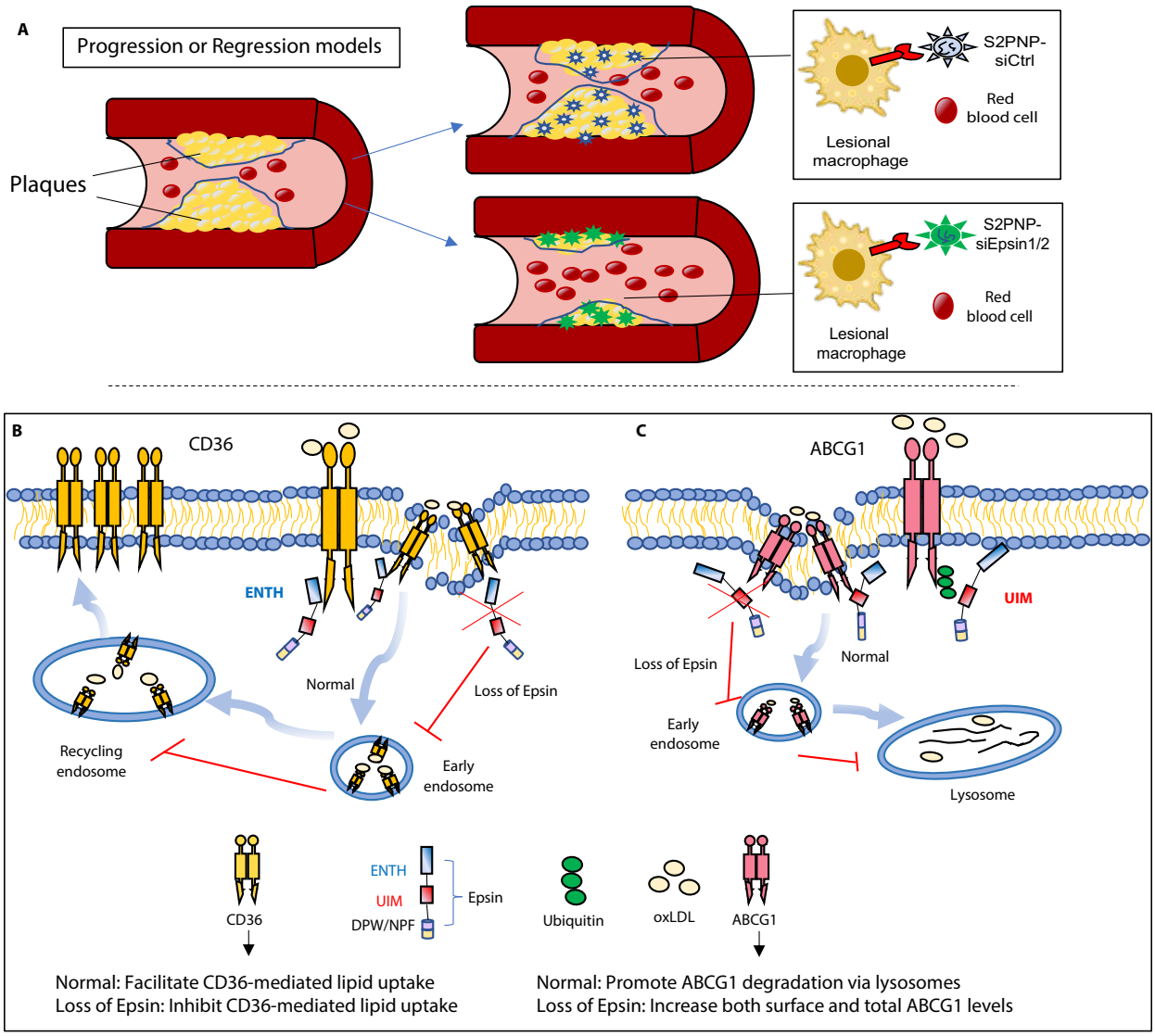
A
Progression or Regression models
Plaques
S2PNP-siCtrl
Red blood cell
Lesional macrophage
S2PNP-siEpsin1/2
Red blood cell
Lesional macrophage
B
CD36
ENTH
Normal
Loss of Epsin
Recycling endosome
Early endosome
C
ABCG1
UIM
Loss of Epsin
Normal
Early endosome
Lysosome
CD36
ENTH
UIM
DPW/NPF
Epsin
Ubiquitin
oxLDL
ABCG1
Normal: Facilitate CD36-mediated lipid uptake
Loss of Epsin: Inhibit CD36-mediated lipid uptake
Normal: Promote ABCG1 degradation via lysosomes
Loss of Epsin: Increase both surface and total ABCG1 levels

841 **Table S1. Demographic Information of The Human Samples**
842

Individual name	Gender	Tissue Source	Normal/ Diseased	Age	Site of Primary Disease 1	Specific Diagnosis 1	Malignant /Benign	Disease Type
RA06-1040	M	Aorta	Diseased	62-83	Aorta	atherosclerosis	Benign	Atherosclerotic lesion
RA06-2816	M	Aorta	Diseased	62-83	Aorta	atherosclerosis	Benign	Atheroscelrotic lesion
RA03-0422	F	Aorta	Diseased	62-83	Aorta	atherosclerosis	Benign	Atherosclerostic plaque with calcifications
RA02-0678	M	Aorta	Diseased	62-83	Aorta	atherosclerosis	Benign	Mild ahterosclerotic change
RA03-0488	M	Aorta	Diseased	62-83	Aorta	atherosclerosis	Benign	Thrombus and atheroscelrotic plaque severe
RA03-0857	F	Aorta	Diseased	62-84	Aorta	atherosclerosis	Benign	Atheroscelrosis with subintimal hemorrhage
RA03-1686	M	Aorta	Normal	<20	Aorta	Dissection	Benign	N/A
R14-0199	M	Aorta	Normal	62-83	Aorta	Dissection	Benign	N/A
RA04-2408	F	Aorta	Normal	62-83	Heart	Degeneration	Benign	N/A

843
844
845 **Table S2. Statistical Table**

Figure	Sample Size (n)	Parametric Analysis Type	P (or adjusted P) Value
2A WT VS DKO-CD36	5	Unpaired non-parametric Mann-Whitney U test	5.5x10^-1
2A WT VS DKO-Epsin1	5	Unpaired non-parametric Mann-Whitney U test	7.9 x10^-3
2A WT VS DKO-Epsin2	5	Unpaired non-parametric Mann-Whitney U test	7.9 x10^-3
2B WT VS DKO -oxLDL	4	Unpaired non-parametric Mann-Whitney U test	9.9x10^-1 (adjusted p value)
2B WT VS DKO +oxLDL	4	Unpaired non-parametric Mann-Whitney U test	2.0x10^-1 (adjusted p value)
2B -oxLDL VS +oxLDL WT	4	Unpaired non-parametric Mann-Whitney U test	4.9x10^-1 (adjusted p value)
2B -oxLDL VS +oxLDL DKO	4	Unpaired non-parametric Mann-Whitney U test	4.9x10^-1 (adjusted p value)
2C WT VS DKO -oxLDL	4	Unpaired non-parametric Mann-Whitney U test	8.9x10^-1 (adjusted p value)
2C WT VS DKO +oxLDL	4	Unpaired non-parametric Mann-Whitney U test	2.9x10^-2 (adjusted p value)
2C -oxLDL VS +oxLDL WT	4	Unpaired non-parametric Mann-Whitney U test	2.9x10^-2 (adjusted p value)
2C -oxLDL VS +oxLDL DKO	4	Unpaired non-parametric Mann-Whitney U test	9.9x10^-1 (adjusted p value)
2D WT VS DKO -oxLDL	8	Two-way ANOVA Sidak post hoc multiple comparison test	9.8x10^-1 (adjusted p value)

2D WT VS DKO +oxLDL	8	Two-way ANOVA Sidak post hoc multiple comparison test	3.1x10^-7 (adjusted p value)
2D -oxLDL VS +oxLDL WT	8	Two-way ANOVA Sidak post hoc multiple comparison test	3.1x10^-7 (adjusted p value)
2D -oxLDL VS +oxLDL DKO	8	Two-way ANOVA Sidak post hoc multiple comparison test	9.7x10^-1 (adjusted p value)
2E WT VS DKO -oxLDL	8	Two-way ANOVA Sidak post hoc multiple comparison test	9.9x10^-1 (adjusted p value)
2E WT VS DKO +oxLDL	8	Two-way ANOVA Sidak post hoc multiple comparison test	2.7x10^-7 (adjusted p value)
2E -oxLDL VS +oxLDL WT	8	Two-way ANOVA Sidak post hoc multiple comparison test	3.0x10^-7 (adjusted p value)
2E -oxLDL VS +oxLDL DKO	8	Two-way ANOVA Sidak post hoc multiple comparison test	9.9x10^-1 (adjusted p value)
2F WT vs DKO	6	Unpaired t test	4.9x10^-8 (adjusted p value)
2G Cho WT VS DKO -oxLDL	6	Two-way ANOVA Sidak post hoc multiple comparison test	9. 9x10^-1 (adjusted p value)
2G Cho WT VS DKO +oxLDL	6	Two-way ANOVA Sidak post hoc multiple comparison test	8.0 x10^-6 (adjusted p value)
2G Cho -oxLDL VS +oxLDL WT	6	Two-way ANOVA Sidak post hoc multiple comparison test	3.8x10^-7 (adjusted p value)
2G Cho -oxLDL VS +oxLDL DKO	6	Two-way ANOVA Sidak post hoc multiple comparison test	1.0x10^-2 (adjusted p value)
2G TG WT VS DKO -oxLDL	6	Two-way ANOVA Sidak post hoc multiple comparison test	9.8 x10^-1 (adjusted p value)
2G TG WT VS DKO +oxLDL	6	Two-way ANOVA Sidak post hoc multiple comparison test	1.2x10^-5 (adjusted p value)
2G TG -oxLDL VS +oxLDL WT	6	Two-way ANOVA Sidak post hoc multiple comparison test	3.0x10^-6 (adjusted p value)
2G TG -oxLDL VS +oxLDL DKO	6	Two-way ANOVA Sidak post hoc multiple comparison test	9.7x10^-1 (adjusted p value)
2H WT vs DKO	6	Unpaired t test	3.9 x10^-12
3A WT vs DKO	4	Unpaired non-parametric Mann-Whitney U test	2.9 x10^-2
3B WT Vector vs WT	4	Kruskal-Wallis Dunn's multiple comparison test	1.1 x10^-2 (adjusted p value)
3B WT Vector vs ΔUIM	4	Kruskal-Wallis Dunn's multiple comparison test	2.6 x10^-1 (adjusted p value)
3B WT Vector vs ΔENTH	4	Kruskal-Wallis Dunn's multiple comparison test	9.9 x10^-1 (adjusted p value)
3E WT Vector vs WT	6	One way ANOVA Tukey's multiple comparison test	9.9 x10^-1 (adjusted p value)
3E WT Vector vs ΔUIM	6	One way ANOVA Tukey's multiple comparison test	4.4 x10^-1 (adjusted p value)
3E WT Vector vs ΔENTH	6	One way ANOVA Tukey's multiple comparison test	9.8 x10^-1 (adjusted p value)
3E DKO Vector vs WT	6	One way ANOVA Tukey's multiple comparison test	8.9 x10^-13 (adjusted p value)

3E DKO Vector vs ΔUIM	6	One way ANOVA Tukey's multiple comparison test	9.1 x10^-13 (adjusted p value)
3E DKO Vector vs ΔENTH	6	One way ANOVA Tukey's multiple comparison test	9.9 x10^-1 (adjusted p value)
5A WT vs DKO	9	One way ANOVA Tukey's multiple comparison test	6.1 x10^-9 (adjusted p value)
5A WT vs DKO/ABCG1 fl/+	9	One way ANOVA Tukey's multiple comparison test	8.9 x10^-3 (adjusted p value)
5A DKO vs DKO/ABCG1 fl/+	9	One way ANOVA Tukey's multiple comparison test	1.0 x10^-6 (adjusted p value)
5B WT vs DKO	9	One way ANOVA Tukey's multiple comparison test	4.3 x10^-1 (adjusted p value)
5B WT vs DKO/ABCG1 fl/+	9	One way ANOVA Tukey's multiple comparison test	7.6 x10^-1 (adjusted p value)
5B DKO vs DKO/ABCG1 fl/+	9	One way ANOVA Tukey's multiple comparison test	8.5 x10^-1 (adjusted p value)
5D WT vs DKO	6	One way ANOVA Tukey's multiple comparison test	1.0 x10^-6 (adjusted p value)
5D WT vs DKO/ABCG1 fl/+	6	One way ANOVA Tukey's multiple comparison test	9.3 x10^-1 (adjusted p value)
5D DKO vs DKO/ABCG1 fl/+	6	One way ANOVA Tukey's multiple comparison test	2.0 x10^-6 (adjusted p value)
5E WT vs DKO	6	One way ANOVA Tukey's multiple comparison test	2.0 x10^-6 (adjusted p value)
5E WT vs DKO/ABCG1 fl/+	6	One way ANOVA Tukey's multiple comparison test	7.1 x10^-1 (adjusted p value)
5E DKO vs DKO/ABCG1 fl/+	6	One way ANOVA Tukey's multiple comparison test	8.0 x10^-6 (adjusted p value)
5F WT vs DKO	6	One way ANOVA Tukey's multiple comparison test	2.2 x10^-3 (adjusted p value)
5F WT vs DKO/ABCG1 fl/+	6	One way ANOVA Tukey's multiple comparison test	9.5 x10^-1 (adjusted p value)
5F DKO vs DKO/ABCG1 fl/+	6	One way ANOVA Tukey's multiple comparison test	4.1 x10^-3 (adjusted p value)
5G WT vs DKO	6	One way ANOVA Tukey's multiple comparison test	2.5 x10^-5 (adjusted p value)
5G WT vs DKO/ABCG1 fl/+	6	One way ANOVA Tukey's multiple comparison test	9.9 x10^-1 (adjusted p value)
5G DKO vs DKO/ABCG1 fl/+	6	One way ANOVA Tukey's multiple comparison test	2.6 x10^-5 (adjusted p value)
5H WT vs DKO	6	One way ANOVA Tukey's multiple comparison test	8.6 x10^-5 (adjusted p value)
5H WT vs DKO/ABCG1 fl/+	6	One way ANOVA Tukey's multiple comparison test	9.9 x10^-1 (adjusted p value)
5H DKO vs DKO/ABCG1 fl/+	6	One way ANOVA Tukey's multiple comparison test	9.6 x10^-5 (adjusted p value)
5I WT vs DKO	6	One way ANOVA Tukey's multiple comparison test	1.4 x10^-5 (adjusted p value)
5I WT vs DKO/ABCG1 fl/+	6	One way ANOVA Tukey's multiple comparison test	5.4 x10^-1 (adjusted p value)

5I DKO vs DKO/ABCG1 fl/+	6	One way ANOVA Tukey's multiple comparison test	9.0 x10^-5 (adjusted p value)
5K WT vs DKO	3	Kruskal-Wallis Dunn's multiple comparison test	9.9 x10^-1 (adjusted p value)
5K WT vs DKO/ABCG1 fl/+	3	Kruskal-Wallis Dunn's multiple comparison test	1.6 x10^-1 (adjusted p value)
5K DKO vs DKO/ABCG1 fl/+	3	Kruskal-Wallis Dunn's multiple comparison test	1.1 x10^-1 (adjusted p value)
5L WT vs DKO	3	Kruskal-Wallis Dunn's multiple comparison test	2.2 x10^-2 (adjusted p value)
5L WT vs DKO/ABCG1 fl/+	3	Kruskal-Wallis Dunn's multiple comparison test	5.4 x10^-1 (adjusted p value)
5L DKO vs DKO/ABCG1 fl/+	3	Kruskal-Wallis Dunn's multiple comparison test	5.4 x10^-1 (adjusted p value)
6A ABCG1 WT vs DKO	4	Unpaired non-parametric Mann-Whitney U test	2.9 x10^-2
6A ABCA1 WT vs DKO	4	Unpaired non-parametric Mann-Whitney U test	6.9 x10^-1
6A SR-A1 WT vs DKO	4	Unpaired non-parametric Mann-Whitney U test	6.9 x10^-1
6A LDLR WT vs DKO	4	Unpaired non-parametric Mann-Whitney U test	6.9 x10^-1
6B ABCG1 WT vs DKO pull	4	Unpaired non-parametric Mann-Whitney U test	2.9 x10^-2
6C (S14B) WT -oxLDL vs +oxLDL 5min	3	Kruskal-Wallis Dunn's multiple comparison test	9.2 x10^-1 (adjusted p value)
6C (S14B) WT -oxLDL vs +oxLDL 15min	3	Kruskal-Wallis Dunn's multiple comparison test	1.2 x10^-1 (adjusted p value)
6C (S14B) WT -oxLDL vs +oxLDL 45min	3	Kruskal-Wallis Dunn's multiple comparison test	6.7 x10^-3 (adjusted p value)
6C (S14B) DKO -oxLDL vs +oxLDL 5min	3	Kruskal-Wallis Dunn's multiple comparison test	3.4 x10^-1 (adjusted p value)
6C (S14B) DKO -oxLDL vs +oxLDL 15min	3	Kruskal-Wallis Dunn's multiple comparison test	9.2 x10^-1 (adjusted p value)
6C (S14B) DKO -oxLDL vs +oxLDL 45min	3	Kruskal-Wallis Dunn's multiple comparison test	9.9 x10^-1 (adjusted p value)
6D WT vs DKO IP	4	Unpaired non-parametric Mann-Whitney U test	2.9 x10^-2
6E Vector vs WT	4	Kruskal-Wallis Dunn's multiple comparison test	7.0 x10^-3 (adjusted p value)
6E Vector vs ΔENTH	4	Kruskal-Wallis Dunn's multiple comparison test	1.9 x10^-1 (adjusted p value)
6E Vector vs ΔUIM	4	Kruskal-Wallis Dunn's multiple comparison test	9.9 x10^-1 (adjusted p value)
6F -oxLDL-MG132 vs -oxLDL+MG132	3	Kruskal-Wallis Dunn's multiple comparison test	9.2 x10^-1 (adjusted p value)
6F -oxLDL-MG132 vs +oxLDL-MG132	3	Kruskal-Wallis Dunn's multiple comparison test	1.2 x10^-1 (adjusted p value)
6F -oxLDL-MG132 vs +oxLDL+MG132	3	Kruskal-Wallis Dunn's multiple comparison test	6.7 x10^-3 (adjusted p value)
6G -oxLDL VS +oxLDL WT	8	Two-way ANOVA Sidak post hoc multiple comparison test	6.0x10^-12(adjusted p value)

6G -oxLDL VS +oxLDL DKO	8	Two-way ANOVA Sidak post hoc multiple comparison test	9.9 x10^-1 (adjusted p value)
6G WT VS DKO -oxLDL	8	Two-way ANOVA Sidak post hoc multiple comparison test	9.0 x10^-1 (adjusted p value)
6G WT VS DKO +oxLDL	8	Two-way ANOVA Sidak post hoc multiple comparison test	1.4x10^-11(adjusted p value)
6H -oxLDL VS +oxLDL WT	8	Two-way ANOVA Sidak post hoc multiple comparison test	7.9 x10^-13(adjusted p value)
6H -oxLDL VS +oxLDL DKO	8	Two-way ANOVA Sidak post hoc multiple comparison test	8.2x10^-1(adjusted p value)
6H WT VS DKO -oxLDL	8	Two-way ANOVA Sidak post hoc multiple comparison test	9.7x10^-1(adjusted p value)
6H WT VS DKO +oxLDL	8	Two-way ANOVA Sidak post hoc multiple comparison test	7.9x10^-13(adjusted p value)
7B Lesion before vs siCtrl NP	6	One way ANOVA Tukey's multiple comparison test	5.9x10^-9 (adjusted p value)
7B before vs siEpsin1/2 NP	6	One way ANOVA Tukey's multiple comparison test	1.4x10^-1 (adjusted p value)
7B siCtrl NP vs siEpsin1/2 NP	6	One way ANOVA Tukey's multiple comparison test	6.5x10^-9 (adjusted p value)
7C BCA before vs siCtrl NP	6	One way ANOVA Tukey's multiple comparison test	2.0x10^-6 (adjusted p value)
7C BCA before vs siEpsin1/2 NP	6	One way ANOVA Tukey's multiple comparison test	8.8x10^-1 (adjusted p value)
7C BCA siCtrl NP vs siEpsin1/2 NP	6	One way ANOVA Tukey's multiple comparison test	3.0x10^-6 (adjusted p value)
7C Root before vs siCtrl NP	6	One way ANOVA Tukey's multiple comparison test	2.9x10^-8 (adjusted p value)
7C Root before vs siEpsin1/2 NP	6	One way ANOVA Tukey's multiple comparison test	2.0x10^-1 (adjusted p value)
7C Root siCtrl NP vs siEpsin1/2 NP	6	One way ANOVA Tukey's multiple comparison test	2.4x10^-7 (adjusted p value)
7D CD68 before vs siCtrl NP	6	One way ANOVA Tukey's multiple comparison test	6.0x10^-9 (adjusted p value)
7D CD68 before vs siEpsin1/2 NP	6	One way ANOVA Tukey's multiple comparison test	5.7x10^-1 (adjusted p value)
7D CD68 siCtrl NP vs siEpsin1/2 NP	6	One way ANOVA Tukey's multiple comparison test	6.0x10^-9 (adjusted p value)
7D a-SMA before vs siCtrl NP	6	One way ANOVA Tukey's multiple comparison test	1.0x10^-6 (adjusted p value)
7D a-SMA before vs siEpsin1/2 NP	6	One way ANOVA Tukey's multiple comparison test	1.5x10^-7 (adjusted p value)
7D a-SMA siCtrl NP vs siEpsin1/2 NP	6	One way ANOVA Tukey's multiple comparison test	5.8x10^-9 (adjusted p value)
7E BCA before vs siCtrl NP	6	One way ANOVA Tukey's multiple comparison test	5.8x10^-9 (adjusted p value)
7E BCA before vs siEpsin1/2 NP	6	One way ANOVA Tukey's multiple comparison test	5.0x10^-1 (adjusted p value)
7E BCA siCtrl NP vs siEpsin1/2 NP	6	One way ANOVA Tukey's multiple comparison test	5.8x10^-9 (adjusted p value)

7E Root before vs siCtrl NP	6	One way ANOVA Tukey's multiple comparison test	5.8x10^-9 (adjusted p value)
7E Root before vs siEpsin1/2 NP	6	One way ANOVA Tukey's multiple comparison test	7.3x10^-1 (adjusted p value)
7E Root siCtrl NP vs siEpsin1/2 NP	6	One way ANOVA Tukey's multiple comparison test	5.8x10^-9 (adjusted p value)
8D Aorta before vs siCtrl NP	6	One way ANOVA Tukey's multiple comparison test	3.3x10^-1 (adjusted p value)
8D Aorta before vs siEpsin1/2 NP	6	One way ANOVA Tukey's multiple comparison test	1.0x10^-6 (adjusted p value)
8D Aorta siCtrl NP vs siEpsin1/2 NP	6	One way ANOVA Tukey's multiple comparison test	1.2x10^-5 (adjusted p value)
8D Root before vs siCtrl NP	6	One way ANOVA Tukey's multiple comparison test	3.8x10^-1 (adjusted p value)
8D Root before vs siEpsin1/2 NP	6	One way ANOVA Tukey's multiple comparison test	2.9x10^-4 (adjusted p value)
8D Root siCtrl NP vs siEpsin1/2 NP	6	One way ANOVA Tukey's multiple comparison test	4.3x10^-3 (adjusted p value)
8D CD68 before vs siCtrl NP	6	One way ANOVA Tukey's multiple comparison test	7.5x10^-2 (adjusted p value)
8D CD68 before vs siEpsin1/2 NP	6	One way ANOVA Tukey's multiple comparison test	1.1x10^-7 (adjusted p value)
8D CD68 siCtrl NP vs siEpsin1/2 NP	6	One way ANOVA Tukey's multiple comparison test	3.0x10^-6 (adjusted p value)
8D a-SMA before vs siCtrl NP	6	One way ANOVA Tukey's multiple comparison test	7.1x10^-5 (adjusted p value)
8D a-SMA before vs siEpsin1/2 NP	6	One way ANOVA Tukey's multiple comparison test	5.8x10^-9 (adjusted p value)
8D a-SMA siCtrl NP vs siEpsin1/2 NP	6	One way ANOVA Tukey's multiple comparison test	5.8x10^-9 (adjusted p value)
8I VCAM-1	6	Unpaired t test	1.6x10^-8 (adjusted p value)
8I ICAM-1	6	Unpaired t test	6.5x10^-9 (adjusted p value)
8I P-selectin	6	Unpaired t test	9.4x10^-8 (adjusted p value)
8I E-selectin	6	Unpaired t test	2.1x10^-8 (adjusted p value)
8J IL-6	4	Unpaired non-parametric Mann-Whitney U test	2.9x10^-2 (adjusted p value)
8J Il-1b	4	Unpaired non-parametric Mann-Whitney U test	2.9x10^-2 (adjusted p value)
8J TNF-a	4	Unpaired non-parametric Mann-Whitney U test	2.9x10^-2 (adjusted p value)
8J MCP1	4	Unpaired non-parametric Mann-Whitney U test	8.9x10^-1 (adjusted p value)
8J iNOS	4	Unpaired non-parametric Mann-Whitney U test	2.9x10^-2 (adjusted p value)
8J IL-10	4	Unpaired non-parametric Mann-Whitney U test	2.9x10^-2 (adjusted p value)

8J Arg-1	4	Unpaired non-parametric Mann-Whitney U test	2.9x10^-2 (adjusted p value)
8J Epsin1	4	Unpaired non-parametric Mann-Whitney U test	2.9x10^-2 (adjusted p value)
8J Epsin-2	4	Unpaired non-parametric Mann-Whitney U test	2.9x10^-2 (adjusted p value)
S9A	6	Unpaired t test	7.0x10^-11(adjusted p value)
S9B	6	Unpaired t test	7.0x10^-11(adjusted p value)
S13-ABCG1	5	Unpaired non-parametric Mann-Whitney U test	6.9 x10^-1(adjusted p value)
S13-Epsin1	5	Unpaired non-parametric Mann-Whitney U test	7.9 x10^-3(adjusted p value)
S13-Epsin2	5	Unpaired non-parametric Mann-Whitney U test	7.9 x10^-3(adjusted p value)
S15A-CD68	6	Unpaired t test	8.8 x10^-7(adjusted p value)
S15A-ABCG1	6	Unpaired t test	2.0 x10^-6(adjusted p value)
S15B-CD68	6	Unpaired t test	3.0 x10^-6(adjusted p value)
S15-ABCG1	6	Unpaired t test	1.5 x10^-7(adjusted p value)
S16B Epsin1	3	Unpaired non-parametric Mann-Whitney U test	1.0 x10^-1(adjusted p value)
S16B Epsin2	3	Unpaired non-parametric Mann-Whitney U test	1.0 x10^-1(adjusted p value)
S16C Epsin1	3	Unpaired non-parametric Mann-Whitney U test	1.0 x10^-1(adjusted p value)
S16C Epsin2	3	Unpaired non-parametric Mann-Whitney U test	1.0 x10^-1(adjusted p value)
S17A	6	Unpaired t test	3.4x10^-10(adjusted p value)
S17B	6	Unpaired t test	1.8x10^-9(adjusted p value)
S18B Epsin1	4	Unpaired non-parametric Mann-Whitney U test	2.9 x10^-2(adjusted p value)
S18B Epsin2	4	Unpaired non-parametric Mann-Whitney U test	2.9 x10^-2(adjusted p value)
S18C Epsin1	5	Unpaired non-parametric Mann-Whitney U test	7.9 x10^-3(adjusted p value)
S18C Epsin2	5	Unpaired non-parametric Mann-Whitney U test	7.9 x10^-3(adjusted p value)
S18E Aorta before vs siCtrl NP	5	Kruskal-Wallis Dunn's multiple comparison test	1.1 x10^-2(adjusted p value)
S18E Aorta before vs siEpsin1/2 NP	5	Kruskal-Wallis Dunn's multiple comparison test	9.9 x10^-1(adjusted p value)
S18E Aorta siCtrl NP vs siEpsin1/2 NP	5	Kruskal-Wallis Dunn's multiple comparison test	4.8 x10^-2(adjusted p value)
S18E Aorta Root before vs siCtrl NP	5	Kruskal-Wallis Dunn's multiple comparison test	7.1 x10^-3(adjusted p value)

S18E Aorta Root before vs siEpsin1/2 NP	5	Kruskal-Wallis Dunn's multiple comparison test	9.9 x10^-1(adjusted p value)
S18E Aorta Root siCtrl NP vs siEpsin1/2 NP	5	Kruskal-Wallis Dunn's multiple comparison test	7.1 x10^-2(adjusted p value)
S19 BCA collagen before vs siCtrl NP	6	One way ANOVA Tukey's multiple comparison test	5.8 x10^-9(adjusted p value)
S19 BCA collagen before vs siEpsin1/2 NP	6	One way ANOVA Tukey's multiple comparison test	9.1 x10^-2(adjusted p value)
S19 BCA collagen siCtrl NP vs siEpsin1/2 NP	6	One way ANOVA Tukey's multiple comparison test	6.0 x10^-9(adjusted p value)
S19 Root collagen before vs siCtrl NP	6	One way ANOVA Tukey's multiple comparison test	7.3 x10^-9(adjusted p value)
S19 BCA collagen before vs siEpsin1/2 NP	6	One way ANOVA Tukey's multiple comparison test	3.7 x10^-5(adjusted p value)
S19 BCA collagen siCtrl NP vs siEpsin1/2 NP	6	One way ANOVA Tukey's multiple comparison test	5.0 x10^-6(adjusted p value)
S19 BCA Elastic before vs siCtrl NP	6	One way ANOVA Tukey's multiple comparison test	5.8 x10^-9(adjusted p value)
S19 BCA Elastic before vs siEpsin1/2 NP	6	One way ANOVA Tukey's multiple comparison test	2.3 x10^-7(adjusted p value)
S19 BCA Elastic siCtrl NP vs siEpsin1/2 NP	6	One way ANOVA Tukey's multiple comparison test	5.8 x10^-9(adjusted p value)
S19 Root Elastic before vs siCtrl NP	6	One way ANOVA Tukey's multiple comparison test	4.4 x10^-8(adjusted p value)
S19 Root Elastic before vs siEpsin1/2 NP	6	One way ANOVA Tukey's multiple comparison test	1.9 x10^-5(adjusted p value)
S19 Root Elastic siCtrl NP vs siEpsin1/2 NP	6	One way ANOVA Tukey's multiple comparison test	5.8 x10^-9(adjusted p value)
S20 TG before vs siCtrl NP	5	Kruskal-Wallis Dunn's multiple comparison test	7.7 x10^-1(adjusted p value)
S20 TG before vs siEpsin1/2 NP	5	Kruskal-Wallis Dunn's multiple comparison test	9.7 x10^-1(adjusted p value)
S20 TG siCtrl NP vs siEpsin1/2 NP	5	Kruskal-Wallis Dunn's multiple comparison test	9.9 x10^-1(adjusted p value)
S20 Cholesterol before vs siCtrl NP	5	Kruskal-Wallis Dunn's multiple comparison test	9.9 x10^-1(adjusted p value)
S20 Cholesterol before vs siEpsin1/2 NP	5	Kruskal-Wallis Dunn's multiple comparison test	9.9 x10^-1(adjusted p value)
S20 Cholesterol siCtrl NP vs siEpsin1/2 NP	5	Kruskal-Wallis Dunn's multiple comparison test	9.9 x10^-1(adjusted p value)
S20 HDL before vs siCtrl NP	5	Kruskal-Wallis Dunn's multiple comparison test	9.9 x10^-1(adjusted p value)
S20 HDL before vs siEpsin1/2 NP	5	Kruskal-Wallis Dunn's multiple comparison test	9.9 x10^-1(adjusted p value)
S20 HDL siCtrl NP vs siEpsin1/2 NP	5	Kruskal-Wallis Dunn's multiple comparison test	9.9 x10^-1(adjusted p value)
S20 non-HDL before vs siCtrl NP	5	Kruskal-Wallis Dunn's multiple comparison test	9.9 x10^-1(adjusted p value)
S20 non-HDL before vs siEpsin1/2 NP	5	Kruskal-Wallis Dunn's multiple comparison test	9.9 x10^-1(adjusted p value)

S20 non-HDL siCtrl NP vs siEpsin1/2 NP	5	Kruskal-Wallis Dunn's multiple comparison test	9.9 x10^-1(adjusted p value)
S21A BCA before vs siCtrl NP	6	One way ANOVA Tukey's multiple comparison test	3.7 x10^-2(adjusted p value)
S21A BCA before vs siEpsin1/2 NP	6	One way ANOVA Tukey's multiple comparison test	4.0 x10^-6(adjusted p value)
S21A BCA siCtrl NP vs siEpsin1/2 NP	6	One way ANOVA Tukey's multiple comparison test	4.9 x10^-4(adjusted p value)
S21B collagen before vs siCtrl NP	6	One way ANOVA Tukey's multiple comparison test	7.2 x10^-1(adjusted p value)
S21B collagen before vs siEpsin1/2 NP	6	One way ANOVA Tukey's multiple comparison test	5.8 x10^-9(adjusted p value)
S21B collagen siCtrl NP vs siEpsin1/2 NP	6	One way ANOVA Tukey's multiple comparison test	5.8 x10^-9(adjusted p value)
S21B Elastic before vs siCtrl NP	6	One way ANOVA Tukey's multiple comparison test	1.2 x10^-2(adjusted p value)
S21B Elastic before vs siEpsin1/2 NP	6	One way ANOVA Tukey's multiple comparison test	7.8 x10^-9(adjusted p value)
S21B Elastic siCtrl NP vs siEpsin1/2 NP	6	One way ANOVA Tukey's multiple comparison test	9.8 x10^-8(adjusted p value)
S21C CCR-7 WT vs DKO	3	Unpaired non-parametric Mann-Whitney U test	1.0 x10^-1(adjusted p value)
S21C Netrin-1 WT vs DKO	3	Unpaired non-parametric Mann-Whitney U test	1.0 x10^-1(adjusted p value)
S21C Sema-3a WT vs DKO	3	Unpaired non-parametric Mann-Whitney U test	1.0 x10^-1(adjusted p value)
S22D Female Aorta before vs siCtrl NP	5	Kruskal-Wallis Dunn's multiple comparison test	1.4 x10^-2(adjusted p value)
S22D Female Aorta before vs siEpsin1/2 NP	5	Kruskal-Wallis Dunn's multiple comparison test	9.9 x10^-1(adjusted p value)
S22D Female Aorta siCtrl NP vs siEpsin1/2 NP	5	Kruskal-Wallis Dunn's multiple comparison test	4.0 x10^-2(adjusted p value)
S22E Female Aorta before vs siCtrl NP	6	One way ANOVA Tukey's multiple comparison test	1.0 x10^-6(adjusted p value)
S22E Female Aorta before vs siEpsin1/2 NP	6	One way ANOVA Tukey's multiple comparison test	9.8 x10^-1(adjusted p value)
S22E Female Aorta siCtrl NP vs siEpsin1/2 NP	6	One way ANOVA Tukey's multiple comparison test	1.0 x10^-6(adjusted p value)
S22F Female Aorta before vs siCtrl NP	6	One way ANOVA Tukey's multiple comparison test	8.2 x10^-1(adjusted p value)
S22F Female Aorta before vs siEpsin1/2 NP	6	One way ANOVA Tukey's multiple comparison test	1.9 x10^-5(adjusted p value)
S22F Female Aorta siCtrl NP vs siEpsin1/2 NP	6	One way ANOVA Tukey's multiple comparison test	5.4 x10^-5(adjusted p value)
S23A siCtrl vs siEpsin1	4	Unpaired non-parametric Mann-Whitney U test	2.9 x10^-2(adjusted p value)
S23A siCtrl vs siEpsin2	4	Unpaired non-parametric Mann-Whitney U test	2.9 x10^-2(adjusted p value)

S23B siCtrl vs siEpsin1/2	8	Unpaired t test	2.8x10^-16(adjusted p value)
S23C siCtrl vs siEpsin1/2	8	Unpaired t test	5.9x10^-16(adjusted p value)
S23D +HDL siCtrl vs siEpsin1/2	9	Unpaired t test	1.0 x10^-6(adjusted p value)
S23D +ApoA1 siCtrl vs siEpsin1/2	9	Unpaired t test	8.1 x10^-1(adjusted p value)
S24E siCtrl vs siEpsin1/2 -oxLDL	5	Unpaired non-parametric Mann-Whitney U test	6.9x10^-1 (adjusted p value)
S24E siCtrl vs siEpsin1/2 +oxLDL	5	Unpaired non-parametric Mann-Whitney U test	7.9 x10^-3(adjusted p value)
S24E -oxLDL VS +oxLDL siCtrl	5	Unpaired non-parametric Mann-Whitney U test	7.9 x10^-3(adjusted p value)
S24E -oxLDL VS +oxLDL siEpsin1/2	5	Unpaired non-parametric Mann-Whitney U test	6.7 x10^-1(adjusted p value)
S24F siCtrl vs siEpsin1/2 -oxLDL	5	Unpaired non-parametric Mann-Whitney U test	8.4x10^-1 (adjusted p value)
S24F siCtrl vs siEpsin1/2 +oxLDL	5	Unpaired non-parametric Mann-Whitney U test	7.9 x10^-3(adjusted p value)
S24F -oxLDL VS +oxLDL siCtrl	5	Unpaired non-parametric Mann-Whitney U test	7.9 x10^-3(adjusted p value)
S24F -oxLDL VS +oxLDL siEpsin1/2	5	Unpaired non-parametric Mann-Whitney U test	2.0x10^-1 (adjusted p value)
S24G siCtrl vs siEpsin1/2 -oxLDL	5	Unpaired non-parametric Mann-Whitney U test	8.4 x10^-1 (adjusted p value)
S24G siCtrl vs siEpsin1/2 +oxLDL	5	Unpaired non-parametric Mann-Whitney U test	7.9 x10^-3(adjusted p value)
S24G -oxLDL VS +oxLDL siCtrl	5	Unpaired non-parametric Mann-Whitney U test	7.9 x10^-3(adjusted p value)
S24G -oxLDL VS +oxLDL siEpsin1/2	5	Unpaired non-parametric Mann-Whitney U test	4.2 x10^-1(adjusted p value)

846